Improving Nanostructured Lipid Carriers activity against *Helicobacter pylori*: development of pH-responsive systems for gastric settings

Sandra Gomes

Dissertation to obtain the Master's Degree in Bioengineering

Supervisor: Paula Parreira (PhD)

I3S – Instituto de Investigação e Inovação em Saúde, Universidade do Porto; BioEngineered Surfaces Group

INEB – Instituto de Engenharia Biomédica, Porto, Portugal

Co-supervisor: M. Cristina L. Martins (PhD)

I3S – Instituto de Investigação e Inovação em Saúde, Universidade do Porto; BioEngineered Surfaces Group

INEB – Instituto de Engenharia Biomédica, Porto, Portugal

ICBAS – Instituto de Ciências Biomédicas Abel Salazar, Universidade do Porto, Porto, Portugal

September 2021

© Sandra Gomes, 2021

Resumo

A *Helicobacter pylori* é uma bactéria Gram-negativa que coloniza o estômago de metade da população mundial. A infeção crónica com esta bactéria pode provocar gastrite crónica, úlceras pépticas e cancro gástrico. Este é o 5º tipo de cancro mais comum e o 4º mais mortal em todo o mundo e tem uma taxa de sobrevivência relativa a 5 anos de 32%. O tratamento atual, baseado em antibióticos, falha em 20% a 40% dos casos, principalmente devido à resistência da *H. pylori* aos antibióticos. Assim, há a necessidade de desenvolver novas terapias sem recurso a antibióticos para erradicar esta bactéria. Para tal, várias abordagens têm sido estudadas nos últimos anos. No entanto, quando transportadas para cenários *in vivo,* apresentam algumas limitações, como baixa biodisponibilidade, o que dificulta a sua implementação como uma nova abordagem terapêutica contra a *H. pylori*. "Nanostructured lipid carriers" (NLC) foram descritas como tendo elevado potencial contra este patogénico gástrico, mas, para alcançar a erradicação total da bactéria, a biodisponibilidade das NLC terá de ser melhorada, nomeadamente aumentando o seu tempo de retenção no estômago. A goma gelana (GG), um polímero aniónico com propriedades mucoadesivas e excelente capacidade de retenção de água, tem sido amplamente estudada como um sistema de entrega.

O objetivo deste trabalho foi desenvolver um sistema de entrega baseado em GG para libertar de forma controlada ao longo do tempo as NLC no ambiente gástrico.

As NLC foram produzidas pelo método de homogeneização a quente e foram caracterizadas quanto ao seu tamanho e potencial zeta. Os hidrogéis de GG foram produzidos dispersando o pó de GG em água a alta temperatura, seguido de processo de gelificação durante o arrefecimento. A sua estabilidade em diferentes valores de pH e o seu comportamento mecânico foram analisados. A distribuição das NLC e a sua libertação dos hidrogéis de GG *in vitro* em diferentes pH foram avaliadas, assim como a sua performance anti-*H. pylori*.

Os resultados demonstraram que, apesar de apresentarem um comportamento dependente do pH e boas propriedades mecânicas, os hidrogéis compostos apenas por goma gelana com baixo grau de acilação (LAGG) não foram capazes de libertar quantidade suficiente de NLC, o que se traduziu na ausência de atividade antimicrobiana. A adição de goma gelana com elevado grau de acilação (HAGG) à estrutura dos hidrogéis não foi suficiente para melhorar a libertação das NLC. Desta forma, é

necessária uma otimização adicional para melhorar a libertação das nanopartículas dos hidrogéis de GG e assim se maximizar o efeito terapêutico das NLC contra a *H. pylori*.

Palavras-chave: *H. pylori*, infeção gástrica, novas terapias, hidrogéis, "nanostructured lipid carriers"

Abstract

Helicobacter pylori is a Gram-negative bacterium that colonizes the stomach of half of the worldwide population. Chronic infection with this bacterium can lead to chronic gastritis, peptic ulcers and gastric carcinoma. This is the 5th most common and the 4th deadliest type of cancer in the world and has a 5-year relative survival rate of 32%. The current treatment, based on antibiotics, fails in 20% to 40% of the cases, mainly due to *H. pylori* antibiotic resistance. Therefore, there is a need to develop new antibiotic free therapies to eradicate this pathogen. For that, several approaches have been studied over the last years. However, when translated to *in vivo* settings, they present some limitations such as poor bioavailability, which hampers their implementation as a new therapeutic approach against *H. pylori*. Nanostructured lipid carriers (NLC) were described as having high potential against this gastric pathogen. Still, to achieve complete bacterial clearance, NLC bioavailability must be improved, namely by increasing their gastric retention time. Gellan gum (GG) is an anionic polymer with mucoadhesive properties and excellent water retention capacity that has been widely studied as a drug delivery system.

The aim of this work was to develop a GG-based delivery system to deliver NLC in gastric settings.

NLC were produced by hot homogenization method and were characterized regarding their size and zeta potential. GG hydrogels were produced by dispersing GG powder in water at high temperatures, followed by the gelation process during cooling. Their stability at different pH and their mechanical behavior were analyzed. The NLC distribution and their *in vitro* release from GG hydrogels in different pH were also studied, as well as the anti-*H. pylori* performance.

Results demonstrated that, although presenting a pH-responsive behavior and good mechanical properties, hydrogels composed only of low acyl gellan gum (LAGG) could not release enough NLC, which was translated in the absence of antimicrobial activity. The addition of high acyl gellan gum (HAGG) to the structure of the hydrogels was not able to improve the NLC release from the hydrogels. Therefore, further optimization is required to improve the nanoparticles release from GG hydrogels and maximize the therapeutic effect of NLC against *H. pylori*.

Keywords: *H. pylori*, gastric infection, new therapies, hydrogels, nanostructured lipid carriers

Acknowledgements

These pages represent not only the work developed in the last months but also the culmination of a journey that started five years ago. This project was a great opportunity to acquire experience in a lab environment but also to grow personally. For that, I would like to thank all of those who help me in this adventure.

First of all, I would like to express my gratitude to my supervisor Paula Parreira. Thank you for all the help, orientation and patience. Your constant availability, all the video calls and all the ideas discussions were fundamental to my development.

I am also grateful to my co-supervisor Cristina Martins for sharing your scientific knowledge and critical vision, essential for the development of this project. Thank you for receiving me in your group and allowing me to grow.

To Dr. Miguel Oliveira, from I3Bs – Research Institute in Biomaterials, Biodegradables and Biomimetics of University of Minho, for providing his expertise in gellan gum and the polymer powder used in this study and to Dr. Cláudia Nunes Pinho, from the Faculty of Farmacy of the University of Porto, for providing indispensable equipment to this work and her knowledge about nanoparticles.

To all my colleagues from the BioEngineered Surfaces Group, thank you for helping me integrate and for all the funny moments that we shared. To the "pyladies" Diana and Rute, a special thank you for all the help, support and company. To my master students' colleagues and friends António, Nela e Inês, it was a pleasure to share the lab and these experience with all of you.

To my closest friends Catarina and Marta, for all the friendship, for always being present when I needed and for all the adventures that we shared and I hope we continue to share.

To Tiago for all the dedication, support and patience. Thank you for of abdicating your time just to watch me work. Thank you for your love and for always believing in me, for giving me the confidence to achieve my goals and follow my dreams. Thank you for everything.

And last but not the least, thank you to my family, specially to my parents for always being present and for the unconditional support and love. Without you none of these would be possible!

Index

Resumo i

Abstract iii

Ackowledgements v

Index vii

List of Figures ix

List of Tables xi

Abbreviations and Symbols xiii

Chapter I - Introduction 1
1.1 - *Helicobacter pylori* overview 1
1.1.1 - *H. pylori* virulence factors 2
1.1.2 - Current therapies 4
1.1.3 - Novel therapies 6
1.2 - Lipid nanoparticles 8
1.2.1 - NLC as delivery systems 10
1.2.2 - NLC to fight *H. pylori* 10
1.3 - Gastroretentive systems 12
1.4 - Gellan gum 13
1.4.1 - Structure and properties of gellan gum 13
1.4.2 - Gellan gum applications 15
1.5 - Aim 18

Chapter II - Materials and Methods 19
2.1 - NLC preparation and characterization 19
2.1.1 - NLC preparation 19
2.1.2 - Coumarin-6 encapsulation efficiency 20
2.1.3 - NLC characterization 20
2.2 - GG hydrogels production and characterization 20
2.2.1 - Hydrogels production 20
2.2.2 - Hydrogels' stability 21
2.2.3 - Hydrogels' mechanical behavior 22
2.2.4 - NLC distribution in the hydrogels 23
2.3 - NLC release from GG hydrogels 23
2.3.1 - Quantification by fluorescence analysis 23
2.3.2 - Quantification by NTA 23
2.4 - Antimicrobial testing 23
2.4.1 - *H. pylori* culture conditions 23
2.4.2 - Effect of GG hydrogels and their extracts on *H. pylori* growth 24

2.5 - Statistical analysis 24

Chapter III - Results 25
3.1 - NLC preparation and characterization 25
3.2 - LAGG hydrogels production and characterization 26
3.2.1 - LAGG hydrogels production 26
3.2.2 - LAGG hydrogels' stability 27
3.2.3 - LAGG hydrogels' mechanical behavior 29
3.2.4 - NLC distribution in LAGG hydrogels 30
3.3 - NLC release from LAGG hydrogels 31
3.3.1 - Fluorescence analysis 31
3.3.2 - Nanoparticle tracking analysis 33
3.4 - Antimicrobial properties of LAGG hydrogels 34
3.5 - Hydrogel optimization to improve NLC release 36
3.5.1 - HAGG:LAGG hydrogels production 36
3.5.2 - HAGG:LAGG hydrogels' stability 36
3.5.3 - HAGG:LAGG hydrogels' mechanical behavior 39
3.5.4 - NLC release from HAGG:LAGG hydrogels 40

Chapter IV - Discussion 43

Chapter V - Conclusion 49

Chapter VI - Future perspectives 51

References 53

List of Figures

Figure 1. Global gastric cancer incidence in 2020 2

Figure 2. Main factors that contribute to the success of the infection by *H. pylori* 3

Figure 3. Structure and composition of lipid nanoparticles 9

Figure 4. Stucture and composition of different types of nanostructured lipid carriers 9

Figure 5. Schematic representation of different gastroretentive systems 13

Figure 6. Chemical structure of gellan gum 14

Figure 7. Schematic representation of the aim of the work..... 18

Figure 8. Schematic representation of NLC production by hot homogenization method..... 19

Figure 9. Schematic representation of LAGG hydrogels production..... 21

Figure 10. Schematic representation of HAGG and HAGG:LAGG hydrogels production 21

Figure 11. Responses measured by DMA technique after stress application 22

Figure 12. NLC characterization..... 25

Figure 13. Coumarin-6 calibrtion curve in water 26

Figure 14. LAGG, NLC-LAGG and cNLC-LAGG hydrogels 26

Figure 15. LAGG hydrogels' diameter..... 27

Figure 16. Stability of LAGG hydrogels in different mediums..... 28

Figure 17. Mechanical behavior of LAGG hydrogels 29

Figure 18. NLC distribution in LAGG hydrogels..... 30

Figure 19. Emission spectrums of free coumarin-6 and coumarin-6-loaded NLC (cNLC) 31

Figure 20. cNLC calibration curves in different pH conditions (different mediums)..... 32

Figure 21. cNLC release from LAGG hydrogels in different mediums..... 32

Figure 22. NLC release from LAGG hydrogels in different mediums 33

Figure 23. Antimicrobial activity of LAGG and NLC-LAGG hydrogels..... 34

Figure 24. Antimicrobial activity of the extracts of LAGG hydrogels 35

Figure 25. HAGG:LAGG hydrogels 36

Figure 26. LAGG 2% (100LAGG), 100HAGG and HAGG:LAGG hydrogels' diameter 37

Figure 27. Stability of LAGG 2% (100LAGG), 100HAGG and HAGG:LAGG hydrogels in different pH conditions 38

Figure 28. 100HAGG hydrogels after pipetting 39

Figure 29. Mechanical behaviour of LAGG 2% (100LAGG), 100HAGG and HAGG:LAGG hydrogels 39

Figure 30. NLC release from LAGG 2% (100LAGG), 100HAGG and HAGG:LAGG hydrogels 40

List of Tables

Table 1. Antibiotic-based treatments to eradicate *H. pylori*.....5

Table 2. Strategies that use NLC as a delivery system to improve compound's oral bioavailability 11

Table 3. Main drawbacks of the different gastroretentive systems 12

Table 4. Gellan gum-based systems in drug delivery applications..... 17

Table 5. Timepoints used for NLC quantification by NTA 23

Table 6. Absolute number of NLC in each LAGG hydrogel's disc 31

Table 7. Number of cNLC released from LAGG hydrogels in different pH conditions..... 33

Table 8. Number of NLC released from LAGG hydrogels in different pH conditions 34

Table 9. Number of NLC in each disc of LAGG 2% (100LAGG), 100HAGG and HAGG:LAGG..... 40

Table 10. Number of NLC released from LAGG 2% (100LAGG), 100HAGG and HAGG:LAGG hydrogels in different pH conditions 41

Abbreviations and Symbols

List of abbreviations

ACG	American College of Gastroenterology
AJCC	American Joint Committee on Cancer
AMPs	antimicrobial peptides
BabA	blood group antigen-binding adhesin
BB	Brucella Broth
CagA	cytotoxicity-associated immunodominant antigen A
CB	citrate buffer
CFU	colony forming unit
cNLC	coumarin-6-loaded nanostructured lipid carriers
DHA	docosahexaenoic acid
DLS	dynamic light scattering
DMA	dynamic mechanical analysis
EE	encapsulation efficiency
ELS	electrophoretic light scattering
FBS	fetal bovine serum
FDA	Food and Drug Administration
GG	gellan gum
HAGG	high acyl gellan gum
IARC	International Agency for Research on Cancer
LAGG	low acyl gellan gum
LDC	lipid-drug conjugates
LL	liquid lipid
LPS	lipopolysaccharide
MIC	minimal inhibitory concentration
NLC	nanostructured lipid carriers
NTA	nanoparticle tracking analysis
OD	optical density
PB	phosphate buffer

PBS	phosphate-buffered saline
PI	polydispersity index
PPI	proton pump inhibitor
PUFAs	polyunsaturated fatty acids
ROS	reactive oxygen species
rpm	revolutions per minute
SabA	sialic acid binding adhesin
SGF	simulated gastric fluid
SL	solid lipid
SLN	solid lipid nanoparticles
SURF	surfactant
VacA	vacuolating cytotoxin A
WHO	World Health Organization

List of symbols

λ	wavelength
v	volume
w	weight

Chapter I – Introduction

1.1. *Helicobacter pylori* overview

Helicobacter pylori is a spiral-shaped microaerophilic[1] Gram-negative bacterium that colonizes the stomach of nearly half of the population around the world [1]. However, infection rates present a wide variability according to the continent and the country being, in general, higher in developing countries than in developed countries, possibly due to poorer sanitation conditions [1-3]. Nonetheless, some developed countries still have alarmingly high infection rates, which is the case of Portugal, with an infection rate superior to 80% [4]. Transmission of *H. pylori* is thought to occur from person-to-person, probably by fecal-oral route or oral-oral route [5] or through contaminated water sources [6]. Also, it has been argued that this bacterium may be transmitted via zoonotic route[2] [7].

Infection with *H. pylori* is silent, as only around 20% of the infected people develop clinical conditions with associated symptomatology, such as chronic gastritis and peptic ulcers [8]. However, chronic infection with this pathogen is responsible for 89% of all non-cardia gastric cancers [9], being *H. pylori* classified in 1994 by the World Health Organization (WHO) and the International Agency for Research on Cancer (IARC) as a Group 1 agent - definite carcinogenic to humans [10]. To date, gastric cancer still ranks as the 5th most common and the 4th deadliest type of cancer worldwide [11] (Figure 1). According to the American Joint Committee on Cancer (AJCC), gastric cancer has different stages according to the degree to which the cancer has spread. In stages 0 and IA, the cancer is localized within the stomach and has not spread outside of it. In more advanced stages like IB, II and III, the cancer has spread to nearby structures or lymph nodes outside the stomach. The latest stage (IV) corresponds to the metastatic phase, where the cancer has spread to distant parts of the body [12]. Since most patients do not present symptoms in the early stages, the diagnosis of gastric cancer is frequently made only when the disease is in advanced stage [13], which impairs the prognosis of the patient. The overall 5-year relative survival rate of gastric cancer is 32%, but it varies widely according to the disease state: if the cancer is localized within the stomach, the survival rate is 70%; if the cancer has already spread to nearby structures, the survival rate decreases to 32% and, if the cancer has metastasized to distant parts of the body, the survival rate is only 6% [14].

[1] A microaerophile is a microorganism that requires environments containing lower levels of oxygen than those that are present in the atmosphere to survive (typically 2-10%; *H. pylori* requires less than 5%).

[2] Zoonotic transmission refers to infectious disease transmission from animals to humans.

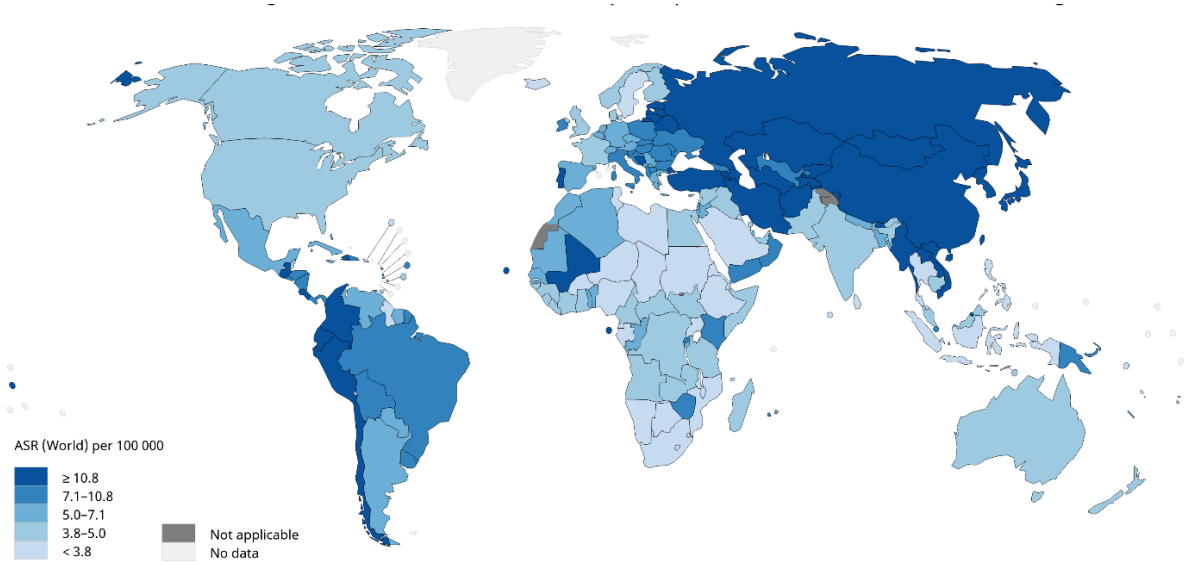


Figure 1. Global gastric cancer incidence in 2020. The estimated incidence rates are age-standardized and include both women and men. Retrieved from GLOBOCAN 2020 [9].

1.1.1. H. pylori virulence factors

H. pylori presents multiple virulence factors that influence its pathogenicity and largely contribute to the infection success (Figure 2).

Bacterial motility is given by its four to eight flagella that, together with chemotaxis mechanisms based on sensing pH variations, allows the bacteria to escape the acidic environment of the gastric lumen [15]. This is crucial for *H. pylori* survival, since it enables the bacteria to cross the mucus layer and reach the gastric epithelium, which has a more neutral pH (Figure 2) [16]. Another mechanism that helps *H. pylori* survival in the harsh acidic environment of the stomach is the secretion of the enzyme urease, which converts endogenous urea to carbon dioxide and ammonia, generating a neutral environment in the bacteria immediate vicinity [16]. Urease also facilitates the colonization of the gastric epithelium, since the action of the enzyme changes the viscoelasticity of the gastric mucus gel layer, which facilitates the movement of the bacteria through this barrier [16]. Moreover, the enzymes phospholipase A and C, present in all strains of *H. pylori*, also enhance infection, as they are involved in the destruction of the phospholipidic components of the protective mucous barrier [17].

For a long-term persistence in the stomach, adhesion to the gastric mucosa is a fundamental feature. For that, *H. pylori* expresses different adhesins that are able to specifically recognize molecules present in the surface of the host cells [18]. This adhesion protects the bacteria from displacement by the forces generated in the stomach during peristalsis and gastric emptying, while also facilitating access to nutrients from the host cells [19, 20]. One of those adhesins is the blood group antigen-binding adhesin (BabA), more specifically the isoform babA2, that binds to Lewis b antigens present in the gastrointestinal mucosa [18]. BabA expression is controlled by phase variation and appears to be associated with the bacterial load [21]. Another adhesin is the sialic acid binding adhesin (SabA) that recognizes sialyl-Lewis X antigens, which are usually present in inflamed cells of the gastric epithelium [18]. Goodwin *et al.* demonstrated that these adhesins have an “on/off”

mechanism. Their expression is controlled by phase variation and by the acid-responsive ArsRS signal transducing system that perceives low-pH, which allows the rapid adaptation of *H. pylori* to varying microenvironments or host immune responses [22].

H. pylori has a lipopolysaccharide (LPS), the major component of the outer membrane of Gram-negative bacteria, that is less proinflammatory than the LPS from other bacteria, which enables to escape host defenses and reach chronic infection status [23]. Furthermore, the *H. pylori* O antigen, a variable carbohydrate chain attached to the lipid A component of the LPS of the bacteria, presents structural homology with molecules present in the human gastric mucosa, namely with the above-mentioned Lewis blood group antigens, being therefore bacteria "camouflaged" from the host immune system [18, 24].

H. pylori produces proteins that can interfere with and damage the host cells, as the cytotoxicity-associated immunodominant antigen A (CagA) protein, which is encoded by the *cagA* gene that is localized in the *cag* pathogenicity island. This pathogenicity island contains other genes that codify, for example, a type IV secretion system that translocates CagA into host cells. Once inside the gastric epithelial cells, this protein induces several alterations in cellular signaling pathways [17, 18]. Other protein that can disrupt host cells is the vacuolating cytotoxin A (VacA), which induces the formation of vacuoles in the cells [25]. Although not all *H. pylori* strains are able to produce both CagA and VacA, those who can (60-70% for CagA and around 50% of *H. pylori* strains for VacA) are more virulent and associated to poorer infection prognosis [17, 18].

Finally, under hostile conditions, *H. pylori* is capable of undergo morphological changes from bacillar to coccoid. Coccoid conformation corresponds to a viable but not culturable state, where the bacteria is in a dormant state with minimal metabolic activity, yet maintaining their virulence factors

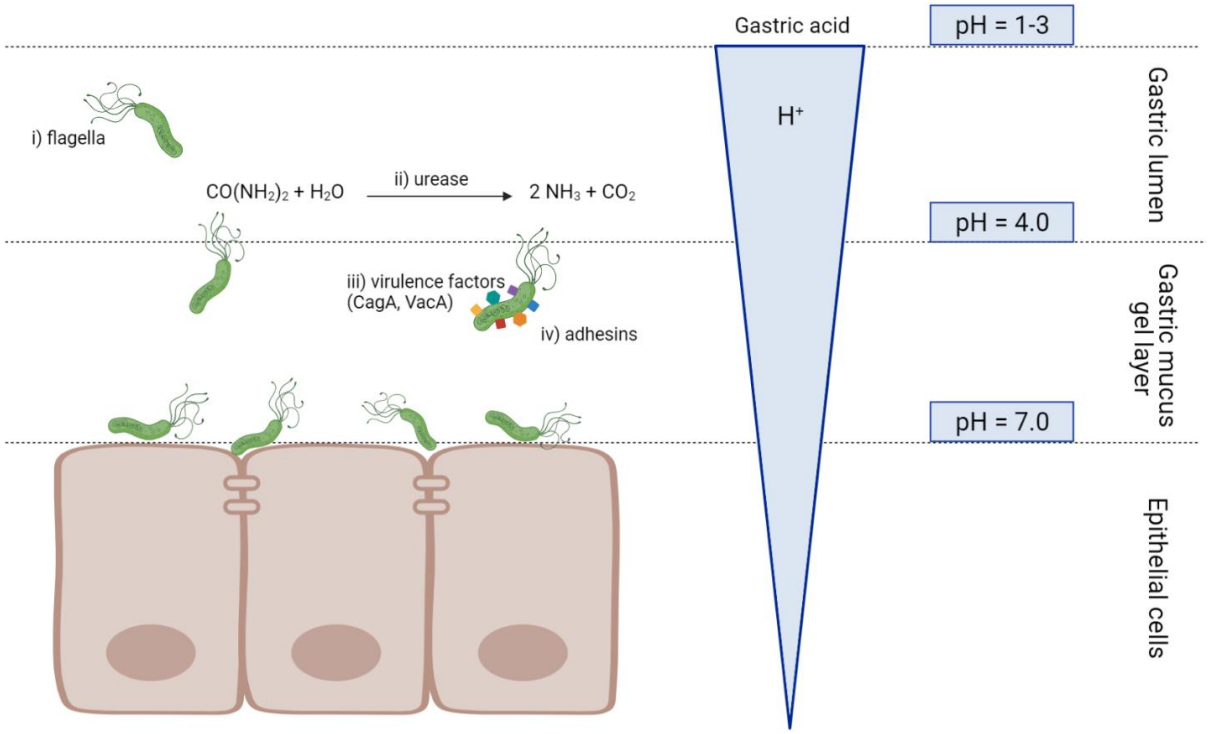


Figure 2. Main factors that contribute to the success of the infection by *H. pylori*. Image created with BioRender software.

active, namely urease, cytotoxic islands and vacuolating toxins. This makes possible the colonization of the gastric mucosa by this form of *H. pylori* [26, 27]. Coccoid conformation favors *H. pylori* survival since it becomes less susceptible to antibiotics [28].

1.1.2. Current therapies

H. pylori eradication from infected people, either symptomatic or not, is nowadays advocated as the best option to avoid the gastric disorders mentioned above, but also to decrease the gastric cancer burden worldwide. Current therapies combine different antibiotics (depending on the regimen) with a proton pump inhibitor (PPI), over 10-14 days (Table 1). The standard regimen, i.e., the one that is more commonly prescribed, is the one based on the clarithromycin triple therapy (a PPI combined with two antibiotics: clarithromycin and amoxicillin or metronidazole). However, it fails in 20%-40% of the cases, mainly due to high antibiotic resistance rates [29]. In fact, in 2017 this bacterium was considered as one of the 16 most threatening bacteria in terms of antibiotic resistance and public health, being classified as a high priority in terms of clarithromycin resistance [30]. This led recent guidelines from Europe, USA and Canada to recommend the use of clarithromycin triple therapy only in regions with low clarithromycin resistance (<15%) [31-33]. When clarithromycin resistance rates are higher, other treatment possibilities are based on bismuth quadruple therapy (a PPI combined with bismuth and two antibiotics: tetracycline and metronidazole) or concomitant therapy (a PPI combined with three antibiotics: clarithromycin, amoxicillin and a nitroimidazole) [31-33]. Other therapeutic regimens that may be used for *H. pylori* eradication are described in Table 1.

Besides the high antibiotic resistance rates, there are other factors that account for the treatment failure, namely: i) poor patient compliance due to the regimens complexity and antibiotics severe side effects, such as taste disturbances and diarrhea [34]; ii) insufficient drug concentration in the infection site, as antibiotics degrade in the acidic environment of the stomach and to the presence of the mucus layer makes it difficult for antibiotics to reach the surface of the gastric epithelial cells where the bacteria are adhered [34] and; iii) patient life style, such as smoking and coffee intake, as well as previous exposure to antibiotics [35, 36].

Table 1. Antibiotic-based treatments to eradicate *H. pylori*. (1x) daily; (2x) twice a day; (3x) three times a day; (4x) four times a day. Data based on the Maastricht V/Florence Consensus [31], American College of Gastroenterology (ACG) [32] and Toronto Consensus [33].

Therapy	Components	Duration	Notes
Clarithromycin triple therapy	PPI standard dose [a] (2x) Clarithromycin 500 mg (2x) Amoxicillin 1 g (2x) OR Metronidazole 500 g (3x)	14 days	First-line therapy in regions with clarithromycin resistance <15%
Bismuth quadruple therapy	PPI standard dose [a] (2x) Bismuth subcitrate 120-300 mg OR subsalicylate 300 mg (4x) Tetracycline 500 mg (4x) Metronidazole 250 mg (4x) OR 500 mg (3x or 4x)	10 - 14 days	First-line therapy; salvage therapy
Concomitant therapy	PPI standard dose [a] (2x) Clarithromycin 500 mg (2x) Amoxicillin 1 g (2x) Nitroimidazole [b] 500 mg (2x)	10 - 14 days	First-line therapy; salvage therapy by ACG
Sequential therapy	(1) PPI standard dose [a] (2x) Amoxicillin 1 g (2x)	5 - 7 days	Conditional first-line therapy by ACG; not recommended by Toronto consensus
	(2) PPI standard dose [a] (2x) Clarithromycin 500 mg (2x) Nitroimidazole [b] 500 mg (2x)	5 - 7 days	
Hybrid therapy	(1) PPI standard dose [a] (2x) Amoxicillin 1 g (2x)	7 days	Conditional first-line therapy by ACG
	(2) PPI standard dose [a] (2x) Amoxicillin 1 g (2x) Clarithromycin 500 mg (2x) Nitroimidazole [b] 500 mg (2x)	7 days	
Levofloxacin triple therapy	PPI standard dose [a] (2x) Levofloxacin 250 mg (2x) OR 500 mg (1x) Amoxicillin 1 g (2x)	10 - 14 days	Conditional first-line therapy by ACG; salvage therapy
Rifabutin triple therapy	PPI standard dose [a] (2x) Rifabutin 150 mg (2x) OR 300 mg (1x) Amoxicillin 1 g (2x)	10 days	Salvage therapy
Fluoroquinolone sequential therapy [c]	(1) PPI Amoxicillin	5 - 7 days	Conditional first-line therapy by ACG; salvage therapy by Maastricht consensus
	(2) PPI Fluoroquinolone Nitroimidazole [b]	5 - 7 days	

[a] The PPI standard dose depends on the PPI used. Standard doses are: esomeprazole 20 mg; lansoprazole 30 mg; omeprazole 20 mg; pantoprazole 40 mg and rabeprazole 20 mg. [b] Metronidazole or tinidazole. [c] No information on the dose of the components.

1.1.3. Novel therapies

Novel therapies that do not rely on antibiotics have been studied as alternatives to the currently available treatments to fight *H. pylori*. The use of different compounds coupled to bioengineered approaches have been widely studied over the last years and some are presented on the next sub-sections.

1.1.3.1. Antimicrobial peptides

Antimicrobial peptides (AMPs) are components of the innate immune system of different species with a broad-spectrum of antimicrobial effect against bacteria, fungi and viruses by interacting with cell membranes [37]. Chen *et al*. demonstrated that Odorranain-HP, a natural AMP identified from skin secretions of diskless odorous frog *Odorrana grahami*, had *in vitro* antimicrobial activity against *H. pylori*, with a minimal inhibitory concentration (MIC) of 20 mg/mL [38]. Pexiganan, an analogue of the magainin peptides isolated from the skin of the African clawed frog *Xenopus laevis* also showed bactericidal effect against the bacteria (Minimal Inhibitory Concentration (MIC) = 2 μg/mL) [39]. Although promising, the *in vivo* use of AMPs can be hampered by proteolysis degradation and peptide aggregation, which implies the use of higher doses, often close to the toxic dosage to achieve the desire efficacy [40]. Immobilization of AMPs is an advocated strategy to help circumvent these obstacles. In a proof-of-concept work, Parreira *et al*. grafted MSI-78A, an AMP derived from MSI-78 (pexiganan), onto model surfaces (self-assembled monolayers, SAMs) to improve the *H. pylori* activity of the peptide. It was observed that the immobilized MSI-78A at a concentration of 30.3±1.2 ng/cm^2 was able to kill 98% of the bacteria after 2h, boosting the antimicrobial activity of this AMP against *H. pylori* [41]. This work further enhanced the usefulness of coupling a bioengineered approach to AMPs.

1.1.3.2. Phytotherapy

Another strategy that has raised interest is phytotherapy, which uses plant-derived bioactive compounds. There is a wide list of natural bioactive compounds with potential as anti-*H. pylori* agents and the mechanisms behind their antimicrobial activity may include urease inhibition, induction of oxidative stress, reduction of *H. pylori* adhesion to the gastric mucosa or protein synthesis inhibition [42]. Parreira *et al*. demonstrated that the extracts of *Eucalyptus* spp. outer bark, mainly composed of triterpenic acids, could inhibit the growth of *H. pylori in vitro* [43]. Olive oil polyphenols also demonstrated *in vitro* activity against the bacteria, especially the secoiridoid aglycons, since they are not hydrolyzed in the acidic environment of the stomach [44]. Mahady *et al*. showed that resveratrol, a polyphenol found in the skin of grapes and other plants, has *in vitro* activity against five different *H. pylori* strains, which may be attributed to the decrease of urease activity when in presence of this compound [45, 46].

Although promising, the use of these compounds as new therapeutic approaches has been delayed by some drawbacks, such as unsuccessful delivery in gastric settings, poor bioavailability,

or low solubility of the compounds. Therefore, the encapsulation of these natural compounds to overcome the mentioned drawbacks may be a useful approach to promote their *in vivo* application in the future.

1.1.3.3. Guided therapies

Guided therapies target specific molecules on the surface of *H. pylori*. Parreira *et al*. showed that both carbohydrate structures Lewis b and sialyl-Lewis x, recognized by *H. pylori* adhesins BabA and SabA respectively, can be identified even when immobilized in model surfaces, which can be promising to use as a decoy to bind and remove *H. pylori* from infected hosts [47]. This was translated by Gonçalves *et al*. to chitosan microspheres designed for oral administration that were decorated with the above mentioned glycans to specifically bind *H. pylori* [48]. These microspheres, that were cross-linked with genipin to endure the acidic pH of the stomach, were able to bind to different *H. pylori* strains under different pH settings. In fact, *in vivo* studies in mice showed that chitosan microspheres alone can reduce the infection rate in 88% [49]. Despite the promising results, this strategy has some limitations, namely the fact that the bacteria are not always expressing those receptors. Also, these are not cost-effective options once translated onto "real-world" scenarios.

Antibodies are other possibility to target specific proteins of *H. pylori*. Gopal *et al*. developed a polyclonal antibody against CagX protein, a component of the type IV secretion system codified by the *cag* pathogenicity island of the bacteria [50]. This can be a promising therapeutic strategy to prevent the correct formation of the secretion system and, therefore, reduce the pathogenicity of *H. pylori*. Ardekani *et al*. used a nanobody to inhibit urease activity, by engineering a single variable domain of the heavy chain antibody against UreC that was able to recognize and bind to these subunit of the enzyme urease, inhibiting its activity [51]. To date, no further *in vivo* studies have been reported regarding this strategy.

1.1.3.4. Polyunsaturated fatty acids

Other bioactive natural compounds that demonstrated excellent antimicrobial performance against *H. pylori* are polyunsaturated fatty acids (PUFAs) [52-54]. Among them, docosahexaenoic acid (DHA), an omega-3 polyunsaturated fatty acid present in fish oil, stood out. DHA inhibited the growth of three *H. pylori* strains *in vitro* by promoting the *H. pylori* transition to the coccoid morphology [55]. Furthermore, *in vivo* studies showed a reduction in the ability of the bacteria to colonize the mouse gastric mucosa in 50% of the infected animals [55]. However, DHA can be easily oxidized due to its highly unsaturated structure, dramatically reducing its bioavailability, which may explain the lack of infection clearance in all animals tested.

Therefore, to improve DHA performance, Seabra *et al*. developed nanostructured lipid carriers (NLC), a type of lipid nanoparticles, to improve the overall antimicrobial activity of DHA against *H. pylori* [56].

In summary, several different strategies are being developed to fight *H. pylori*. Still, what all have in common, is that the coupling to bioengineered approaches may boost their potential/ bioavailability and ultimately improve their performance. In this context, lipid nanocarriers present themselves as one of the most advantageous resources and will be further explored on this Dissertation.

1.2. Lipid nanoparticles

Different types of lipid nanocarriers have been studied for the delivery of bioactive compounds, such as liposomes, (nano)emulsions and lipid micro/nanoparticles. The first lipid nanoparticles to emerge, named solid lipid nanoparticles (SLN), were developed in the beginning of the 1990s by Müller [57] and Gasco [58] to overcome the limitations of existing carrier systems (liposomes, emulsions and polymeric nanoparticles). Regarding polymeric nanoparticles, the polymers may present cytotoxicity after cellular internalization and they lack a suitable method for large scale production [59]. On the other hand, liposomes and emulsions have poor physical stability, may contain residual contaminations due to the use of organic solvents in the production process and have high production costs (in the case of liposomes) [60, 61]. The basic components of SLN are solid lipids (SL), i.e., lipids that are solid at both room and body temperature, and a surfactant (SURF) (Figure 3), but they can also contain other elements such as cryoprotectants, charge modifiers and preservatives [62]. These nanoparticles present multiple advantages such as the capacity to incorporate both hydrophilic and hydrophobic molecules, controlled release of the incorporated compounds, easy scale-up, production methods that do not require the use of organic solvents, good physical stability, and ability to protect labile compounds from degradation [59, 63]. However, they also have some drawbacks, such as poor loading capacity for several substances and expulsion of the encapsulated compound during storage [62, 64]. After production, the lipids that constitute the SLN crystalize in less stable polymorphic forms (α and β' forms) and, during storage, they suffer a polymorphic transition to a more stable form (β form), which results in a more perfect crystalline matrix that expels the incorporated compounds, as described by Westesen *et al*. [65].

Nanostructured lipid carriers (NLC), the second generation of lipid nanoparticles, appeared to overcome the limitations presented by SLN. For that, a liquid lipid (LL) was added to the composition of the nanoparticle (Figure 3), resulting in a less ordered matrix, which increased the particle's loading capacity but also avoided the expulsion of the incorporated substances during storage. The matrix of these nanoparticles remains solid at room and body temperature, like SLN [66]. According to their composition, NLC can be classified in three different types: type I - imperfect; type II -

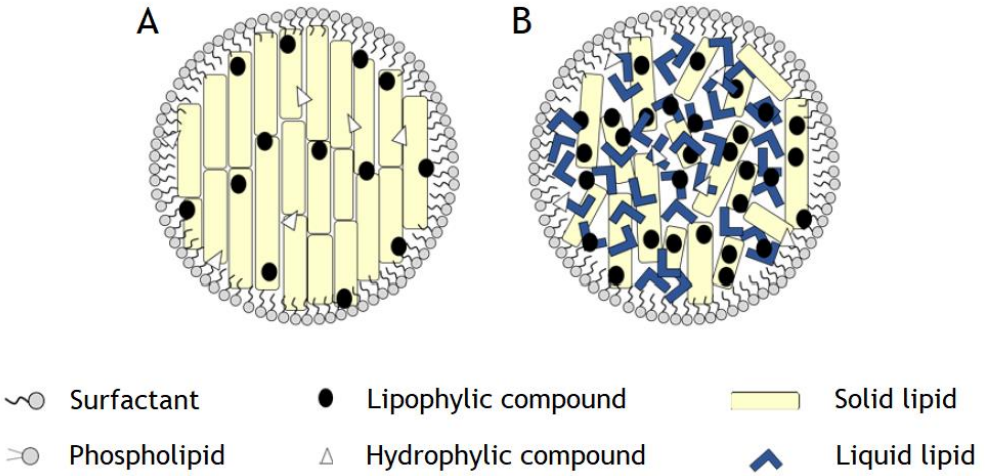


Figure 3. Structure and composition of lipid nanoparticles. (A) SLN; (B) NLC. Adapted from Haider *et al*. [67].

amorphous and type III - multiple [67]. In NLC type I (imperfect type), structurally different lipids (i.e., with different length and saturation of the fatty acid chains) are mixed to produce imperfections in the matrix (Figure 4). Those imperfections generate more space to accommodate the bioactive compound, which increases the loading capacity of the nanoparticles [66, 67]. In NLC type II (amorphous type), a non-crystalline matrix is obtained by mixing a solid lipid with liquid lipids that solidify in an amorphous state (Figure 4), such as hydroxy octacosanyl hydroxyl stearate and isopropyl myristate or triglycerides with a medium chain, like Miglyol-812 [66, 68]. Finally, NLC type III (multiple type) uses the fact that, in general, the solubility of the bioactive compounds is higher in liquid lipids when compared to solid lipids to increase the loading capacity of the nanoparticles (Figure 4). A high amount of liquid lipids is used, exceeding the solubility limit, which leads to the formation of oil nanocompartments that can accommodate large quantities of the molecule to be encapsulated [67, 69].

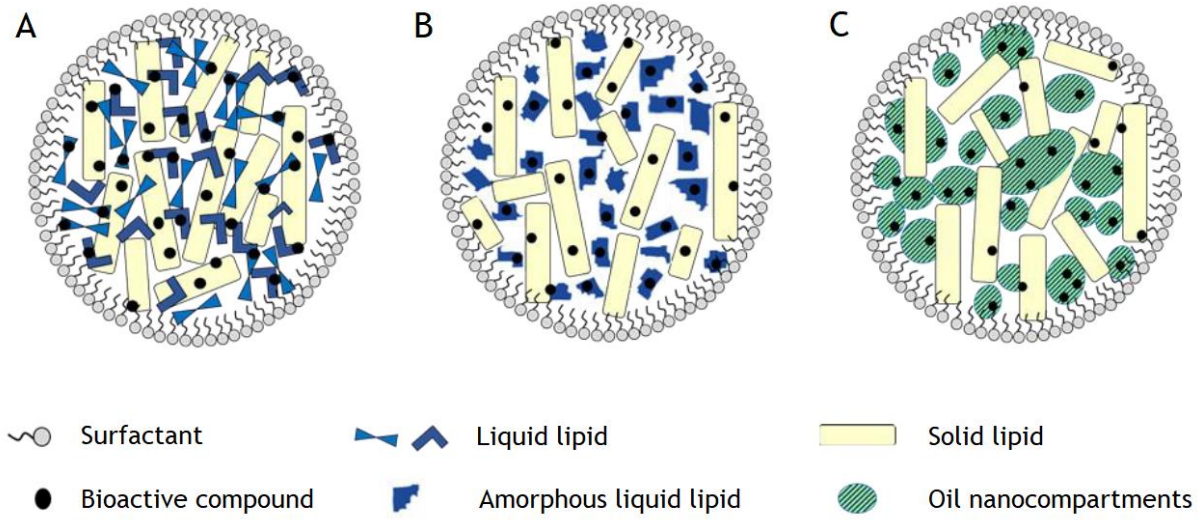


Figure 4. Structure and composition of different types of nanostructured lipid carriers. (A) Imperfect type; (B) Amorphous type; (C) Multiple type. Adapted from Haider *et al*. [67].

Since both SLN and NLC are more suitable for the encapsulation of hydrophobic compounds, a third type of lipid nanoparticles, lipid-drug conjugates (LDC), was developed to improve the encapsulation of hydrophilic bioactive compounds. The hydrophilic compounds are conjugated with a lipidic molecule, leading to the formation of more insoluble and lipophilic molecules. The conjugation can be performed by covalent linkage or by salt formation [70, 71].

Taking all in consideration, NLC are promising lipid carriers to encapsulate bioactive compounds, especially hydrophobic molecules.

1.2.1. NLC as delivery systems

NLC have been widely studied as a delivery system to improve the performance of several different bioactive compounds. For instance, NLC have been used in dermal/topic applications taking advantage of resveratrol potential in the treatment of skin pathologies [72]. Also, the *in vitro* skin permeation of methotrexate, used for the treatment of psoriasis, was increased by its encapsulation into NLC [73]. Besides topical applications, NLC have been studied for other uses and administration routes, namely ocular administration [74], inhalation [75] and intravenous delivery of β-Elemene, a natural compound with anti-cancer activity [76]. Several studies have also used NLC as a delivery system for oral administration of different bioactive compounds, therefore improving its bioavailability. Some are summarized in Table 2.

1.2.2. NLC to fight H. pylori

Seabra *et al*. used NLC to encapsulate DHA (hydrophobic bioactive compound) and improve its antimicrobial performance against *H. pylori* [56]. Surprisingly, NLC alone (placebo) were also effective against *H. pylori*, although requiring more time to kill the bacteria [56]. The NLC bactericidal effect is thought to be associated with physical interactions with the bacterium membrane, which leads to the leakage of cytoplasmatic content and consequent bacterial death [56]. Moreover, it was also observed that these nanoparticles, both DHA-loaded and unloaded, did not affect the gut microbiota [77], a huge feature when compared to the conventional antibiotics, which promote dysbiosis. Still, despite the promising results obtained *in vitro*, the *in vivo* tests showed that DHA-loaded NLC were capable to completely eradicate *H. pylori* in only 50% of the infected animals (Seabra *et al.*, manuscript in preparation). It was also observed that *ad libitum* administration of the NLC (DHA-loaded and unloaded) had better outcome than when administration was done via oral gavage to the animals (Seabra *et al.*; manuscript in preparation). Therefore, to improve the *in vivo* performance, a possible strategy is to increase the NLC bioavailability, namely by increasing their retention time in the stomach, which can be accomplished by using gastroretentive systems.

Table 2. Strategies that use NLC as a delivery system to improve compound's oral bioavailability. In the cases where more than one formulation was tested, NLC components and size refer to the optimal formulation.

Bioactive compound	NLC components	Size (nm)	Research outcomes	Ref
Fenofibrate	**SL** Compritol 888 ATO **LL** Labrafil M 1944CS **SURF** Soya lecithin + Tween 80	84.9 ± 4.9	*In vitro* bi-phasic release pattern (burst release followed by a sustained release) NLC increased by 4 times the compound's concentration in plasma and bioavailability	[78]
Montelukast	**SL** Precirol ATO5 **LL** Capryol-90 **SURF** CAE	181.4 ± 6.5	*In vitro* sustained release from NLC over 24 h It was observed a 143-fold increment in the bioavailability of the compound when encapsulated in the NLC, as compared to the compound aqueous solution	[79]
Vinpocetine	**SL** Compritol 888 ATO **LL** Miglyol 812N **SURF** Solutol HS-15	136 ± 4.2	*In vitro* sustained release profile over 48 h Increase of 3.2 times in the bioavailability by NLC when compared to the compound suspension	[80]
Iloperidone	**SL** Lauric acid **LL** Phosal 53 MCT **SURF** Tween 80 + Poloxamer 188	160.1 ± 3.2	NLC improved the *in vitro* release when compared to the pure compound Bioavailability was increased in 8.3 times	[81]
Atorvastatin	**SL** Gelurice 43/01 **LL** Capryol PGMC **SURF** Lecithin + Pluronic F68	162.5 ± 12	A 3.6- and 2.1-fold increase in bioavailability in comparison to atorvastatin suspension and the commercial product (Lipitor®), respectively, was observed Serum lipid profiles demonstrated that the system has the potential to lower hyperlipidemia	[82]
Raloxifene hydrochloride	**SL** Glyceryl behenate **LL** Oleic acid **SURF** Poloxamer 407	120 ± 3	*In vitro* bi-phasic release profile NLC increased by 3.1 times the compound's bioavailability	[83]
Oleuropein	**SL** Precirol ATO5 **LL** Olive oil **SURF** Tween 80 + Poloxamer 188	141.2 ± 12.3	NLC improved both anti-inflammatory and antioxidant activities *in vitro* (increased the suppression of TNF-α production from J774 macrophages and enhanced reactive oxygen species (ROS) scavenging activity) Oleuropein-loaded NLC reduced ROS generation *in vivo*	[84]

1.3. Gastroretentive systems

Gastroretentive systems are designed to encapsulate and transport therapeutic/bioactive agents, protecting them from the acidic environment of the stomach and, consequently, decreasing their degradation rate. Furthermore, gastroretentive systems use different mechanisms to increase the residence time in the stomach of the encapsulated agents, which also increases their bioavailability [85, 86].

There are different types of gastroretentive systems, namely expandable, bioadhesive, floating, high-density and magnetic systems.

Briefly, expandable systems (Figure 5A) increase their volume when in contact with the gastric fluid to prevent them from passing the pyloric sphincter, which has a mean diameter of 12.8 mm in humans [87]. The increase in volume can be achieved by two different mechanisms, either: a) swelling, which occurs due to water adsorption on hydrophilic polymers or by using smart polymers that change their swelling behavior in response to different stimuli, as pH-responsive systems [86]; or b) by unfolding, where a gastroretentive system with mechanical shape memory is encapsulated in a carrier that, when in contact with the gastric fluid, is degraded, being the gastroretentive system released and acquiring its initial shape [88]. Bioadhesive systems (Figure 5B) use bioadhesive polymers, such as Carbopol [89], chitosan [90] or gellan gum [91], to adhere to biological membranes [86]. Some systems, namely the floating and the high-density systems, have in consideration the density of the gastric fluid. On one hand, floating systems (Figure 5C) present a density lower than the one of the gastric fluid (1.004 g/cm^3), which makes them buoyant [92], while on the other hand, high-density systems (Figure 5D) have a density higher than the gastric fluid, between 2.4 and 2.8 g/cm^3 [93], which makes them sink. Finally, magnetic systems (Figure 5E) use an internal magnet (a component of the dosage form) and an external magnet to retain the system in the stomach [94]. The main drawbacks of each gastroretentive system are summarized in Table 3.

Table 3. Main drawbacks of the different types of gastroretentive systems. Based on Adebisi *et al*. [85] and Lopes *et al*. [86].

Gastroretentive system	Drawbacks
Expandable systems	• Maintenance problems due to the use of hydrolysable and biodegradable polymers • May cause gastric obstruction
Bioadhesive systems	• Constant renewal of the mucus layer • High hydration of the stomach reduces the adhesiveness • Can adhere to other membranes outside the stomach
Floating systems	• Highly dependent on the presence of gastric contents • Require high levels of gastric fluid on the stomach • Lag time until reaching fluctuation
High-density systems	• Difficult to manufacture • Require substantial amount of the active agent
Magnetic systems	• Can be uncomfortable • The external device needs to be precisely located

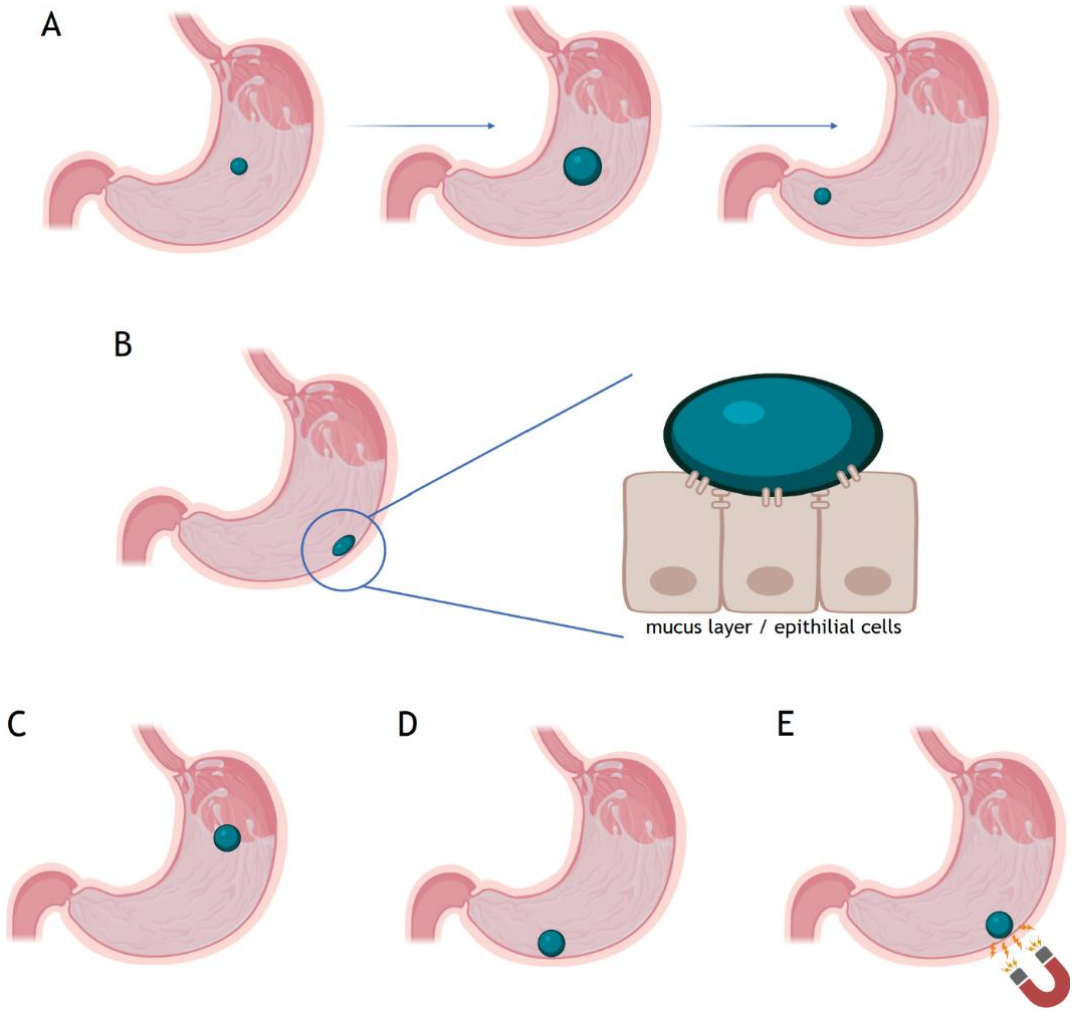


Figure 5. Schematic representation of different gastroretentive systems. (A) Expandable system; (B) Bioadhesive system; (C) Floating system; (D) High-density system and (E) Magnetic system. Image created with BioRender software.

Since the stomach has a wide range of pH values (Figure 2), pH-responsive systems may be a good strategy to increase the gastric retention time of our previously developed NLC (either unloaded or loaded with DHA) to improve their bioavailability and, consequently, their *in vivo* performance. A polymer that can be used for that purpose is gellan gum.

1.4. Gellan gum

1.4.1. Structure and properties of gellan gum

Gellan gum (GG) is a linear anionic exopolysaccharide produced by *Sphingomonas elodea*. GG is approved by the Food and Drug Administration (FDA) as a food additive for human consumption [95]. It is a mucoadhesive, biodegradable, biocompatible and non-cytotoxic polymer that has excellent water retention capacity and is resistant to enzymatic activity [96], namely to pepsin and bile salts [97].

In its native form, also called high acyl gellan gum (HAGG), it is composed of four repeating units (1,3-β-D-glucose, 1,4-β-D-glucuronic acid, 1,4-β-D-glucose and 1,3-α-L-rhamnose) and two acyl substituents, a glycerate and an acetate (Figure 6). These substituents can be removed from the structure by a thermal treatment with alkali, forming low acyl gellan gum (LAGG), the deacylated form of GG [98].

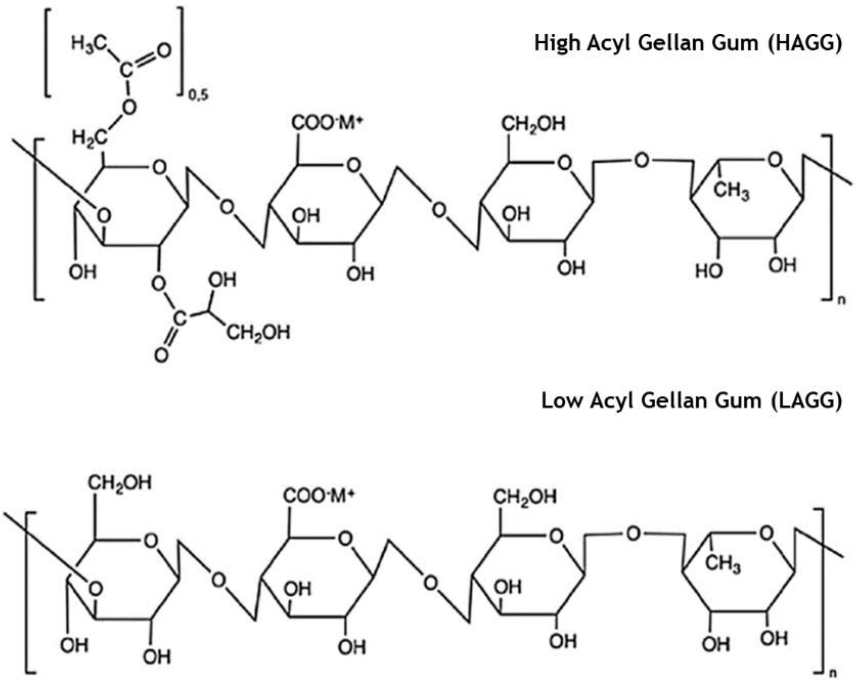


Figure 6. Chemical structure of gellan gum. From Palumbo *et al*. [99].

To obtain a homogeneous dispersion, GG needs to be heated. During the cooling process, a conformational transition from random coil to double helix occurs, leading to the gelation of the polymer. This gelation process undergoes in the presence of cations, as they reduce the electrostatic repulsions between the negatively ionized carboxylate groups of GG, allowing the aggregation of double helices and the formation of a three-dimensional structure [96]. The gelation process is mainly influenced by three aspects: the acylation degree of the polymer, the type and concentration of the ions present in the solution and the pH of the dissolution medium. Regarding the acylation degree, the acyl groups of HAGG cause a less effective packing of the polymer chains, which result in more soft and elastic hydrogels. On the other hand, LAGG presents a more effective packing, resulting in more harder and brittle hydrogels with higher thermal stability [96]. The acylation degree also influences the gelation temperature, being around 65ºC for HAGG and circa 40ºC for LAGG [100]. Concerning the ions type and concentration, higher amounts and/or bigger cations provoke a higher reduction in the electrostatic repulsions and, consequently, gelation and gel strength are enhanced [96]. Finally, harder hydrogels are formed in lower pH values since the electrostatic repulsions are reduced, increasing the chains packing [101].

Some properties of the GG hydrogels, like mass loss and swelling ratio, can be fine-tuned by mixing HAGG and LAGG [102]. Also, GG presents a pH-responsive behavior, with higher swelling behavior at more neutral pH due to the repulsion between the negatively charged carboxyl groups present in the

structure of the polymer [96]. However, it is possible to obtain higher swelling ratios at more acidic mediums by mixing other components to the GG. For instance, Arjama *et al*. combined GG with rice bran albumin and sericin, a protein that contains amino acids that are sensitive to pH, [103], while Mehnath *et al*. combined GG with chitosan, maleic anhydride and sericin [104] to obtain a higher swelling ratio at more acidic pH when compared to more neutral ones. The mucoadhesive properties of the polymer are also influenced by the pH of the medium: GG can establish stronger and more stable polymer networks with mucins at pH 1.2 when compared to pH 6.8, reinforcing GG fitness for gastric settings [91].

1.4.2. Gellan gum applications

GG has been widely studied in the last decades for application in several areas, which will be briefly highlighted over the next sub-sections.

1.4.2.1. Tissue engineering

GG-based matrices can be used to deliver cells to traumatic injuries. A peptide-modified GG hydrogel (using a fibronectin-derived synthetic peptide) was developed to improve stem cells survival for transplantation to treat traumatic spinal cord injuries. The modified hydrogel was able to improve both the adhesion and proliferation of the neural stem/progenitor cells, which may be advantageous in regenerative medicine strategies based in cell transplantation to boost tissue repair after spinal cord injury [105]. GG can also be used in cartilage repair applications. Cartilage repair can be improved by the delivery of stem/progenitor cells and growth factors. GG hydrogels can be used to encapsulate and transport these components. Ahearne *et al*. evaluated the impact of three different hydrogels (gellan gum, fibrin and agarose) in the ability of progenitor cells, together with the TGF-β3 growth factor, to form cartilage. When compared to fibrin and agarose hydrogels, GG hydrogels presented higher cell proliferation and collagen synthesis and concluded that GG hydrogels appear as a promising strategy to deliver cells and growth factors for cartilage repair applications [106]. Hydrogels based on GG were also studied as bone formation platforms. López-Cebral *et al*. developed GG-based hydrogels to deliver the growth factor rhBMP-2. These hydrogels were biocompatible and promoted the attachment and proliferation of C2C12 cells *in vitro*. *In vivo* analysis showed a higher control over the release of the growth factor by the developed hydrogels when compared the commercially available collagen matrices currently used for regenerative purposes. GG hydrogels also presented better tissue integration, which makes these hydrogels a promising strategy for bone regeneration applications [107].

1.4.2.2. Drug delivery

Gellan gum can be used as a drug delivery system in a variety of administration routes. Bhattacharya *et al*. developed GG microbeads for the oral delivery of tranexamic acid, an anti-

fibrinolytic drug, to protect it from the acidic environment of the stomach. The results showed that the microbeads provided intestinal specific controlled released of the compound, which is fundamental to improve its bioavailability [108]. *In situ* GG gels were developed for the sustained ocular delivery of brinzolamide, a drug used to treat high pressure in the eyes. The developed gels were clear and presented an acceptable pH for ocular preparations. Moreover, they had good viscosity that allowed the liquid drops to rapidly undergo a solution-gel transition due to ionic interactions. *In vivo* studies showed that the developed *in situ* gel was less irritating than the drug solution and the commercially available eye drops. Also, it presented a prolonged intraocular pressure-lowering effect after administration [109]. GG-based delivery systems can also be applied to nasal or transdermal routes. Table 4 summarizes some GG-based systems used for drug delivery via different routes.

1.4.2.3. Others

Besides tissue engineering and drug delivery applications, GG is widely use in other areas, such as food industry, reinforcing its safety profile. Kiani *et al*. evaluated the use of GG to extend the shelf-life of doogh, a traditional Iranian drink [110]. Danalache *et al*. used GG as a texturizer in mango bars production [111]. Also, the use of GG, together with sodium alginate, as a water-resistance film coating for paper cups was analyzed [112]. GG has also been studied as a dental filling [113], a component of gels that aim to encapsulate cleaning agents to clean paper artworks [114] and is intensively used in both food and cosmetics industry as a stabilizer to prevent the separation of water and oil in the emulsions [115, 116].

Considering the pH-responsive swelling behavior and the mucoadhesive properties of GG, as well as the promising results obtained for drug delivery in the stomach using GG-based systems [117-120] combined with its biocompatibility and versatile profile, this polymer seems to be a capable system to enhance NLC (unloaded or DHA-loaded) bioavailability in the stomach, by releasing them in a sustained and controlled manner.

Table 4. Gellan gum-based systems in drug delivery applications.

Administration route	Therapeutic agent	Research outcomes	Ref
Oral	Insulin	GG microparticles coated with starch and pectin were developed to enhance the oral delivery of insulin. The microparticles protected insulin from enzymatic degradation and improved its permeability on Caco-2 cells. The *in vitro* release was higher in pH corresponding to the colon when compared to gastric and duodenal pH. *In vivo* studies showed a reduction of up to 51% of blood glucose levels in diabetic rats.	[121]
	Ofloxacin	GG/poly vinyl alcohol nanofibers were developed to improve ofloxacin retention time and bioavailability in the stomach. The nanofibers presented a biphasic release profile in simulated gastric medium and improved the antimicrobial activity against the tested microorganisms. The system presented great *in vitro* mucoadhesive properties and *in vivo* gastric retention in rat's gastric mucosa.	[122]
	Metformin	GG/tamarind seed polysaccharide beads were developed to deliver metformin. *In vitro* release was slower in acidic gastric pH when compared to alkaline intestinal pH. The beads presented good *ex vivo* mucoadhesive properties in goat intestinal mucosa and *in vivo* pharmacodynamic studies showed a sustained reduction in the glucose levels of diabetic rats over 10 h, contrarily to the pure drug.	[123]
Ocular	Olopatadine	GG/Carbopol *in situ* gel was developed to improve the bioavailability of olopatadine. The developed gel was clear, isotonic and presented high *in vitro* gelling capacity. *Ex vivo* studies showed a significant protection of the mast cells from degranulation by the developed formulation. *In vivo* analysis demonstrated that the *in situ* gel are nonirritant and had a prolonged released comparing to eye drop solution. Moreover, the retention time of the gel was higher than both eye drop solution and a commercially available gel.	[124]
	Ofloxacin	Poly(lactide-co-glycolide) (PLGA) microspheres were loaded into GG *in situ* gel to improve corneal penetration and bioavailability of ofloxacin. It was observed an immediate gelation of the formulation after contact with simulated tear fluid. The developed formulation improved the sustained release profile of the drug and increased the *in vivo* bioavailability by almost 12 times in comparison to the commercially available ofloxacin eye drops.	[125]
Nasal	Salbutamol sulphate	GG/hydroxypropyl methyl cellulose mucoadhesive *in situ* gel was developed to deliver salbutamol sulphate. The formulation presented a pH in the range of the nasal cavity pH and an immediate gelation in physiological conditions that remained for an extended period. Drug release was set at 97.34% after 11 h. It was observed an increase in mucoadhesiveness and *ex vivo* permeation in sheep nasal mucosa when compared to the control group.	[126]
	Saquinavir mesylate	GG *in situ* gel was developed to deliver saquinavir mesylate-loaded nanosized microemulsions to improve drug's bioavailability. The system presented good gelling capacity and gel strength and 85% of the drug was released after 12 h. It was observed a 6.5-fold increase in the *ex vivo* permeation percentage comparing to aqueous solution and a 12-fold increase in the bioavailability when compared to commercially available tablets.	
Vaginal	Clindamycin	GG/hydroxypropyl methylcellulose *in situ* gel was developed to prolong residence time of the drug in the infection site. The developed formulation was nonirritant, transparent, had a pH in the range of vaginal pH and presented good mucoadhesive properties. The gelation occurred at physiological conditions and a bi-phasic release pattern was observed with 98.9% of the drug being released after 12 h. Moreover, the formulation presented antimicrobial activity and was stable up to 3 months.	[127]
Transdermal	Diclofenac	GG formulations were developed to enhance skin permeation of diclofenac. The formulations increased the drug skin permeation when compared to commercially available diclofenac topical gel and presented a temperature dependent sustained release up to 24 h.	[128]

1.5. Aim

Novel therapies that do not rely merely on antibiotics to fight *H. pylori* are required. Previously, our team demonstrated that both unloaded and DHA-loaded NLC, were efficient in eradicating the bacteria *in vitro*, although with different time-to-kill kinetics, being DHA-NLC quicker. However, the *in vivo* performance of NLC still requires improvement, as full eradication was achieved in only 50% of the animals subjected to treatment. Also, *ad libitum* administration yielded better results than once a day oral gavage of NLC. As such, the use of gastroretentive systems may allow increasing the NLC's gastric retention time and ultimately enhance their bioavailability and consequent therapeutic effect. GG, besides being widely used in different industries for human consumption attesting its safety and as a drug delivery system for different drugs, has also demonstrated to have a pH-responsive behavior, which fits its use as a NLC's delivery system to the stomach.

Therefore, the main aim of this work was to develop a GG-based delivery system for gastric settings to improve NLC bioavailability, ultimately boosting their *in vivo* performance against *H. pylori*. Ideally, this system would allow the continuous and prolonged release of NLC, which would cross the gastric mucus layer and reach the epithelial cells, where they would exert their bactericidal effect against *H. pylori* (Figure 7). In this work, different formulations of GG hydrogels were designed and tested to obtain the better construct for the intended application.

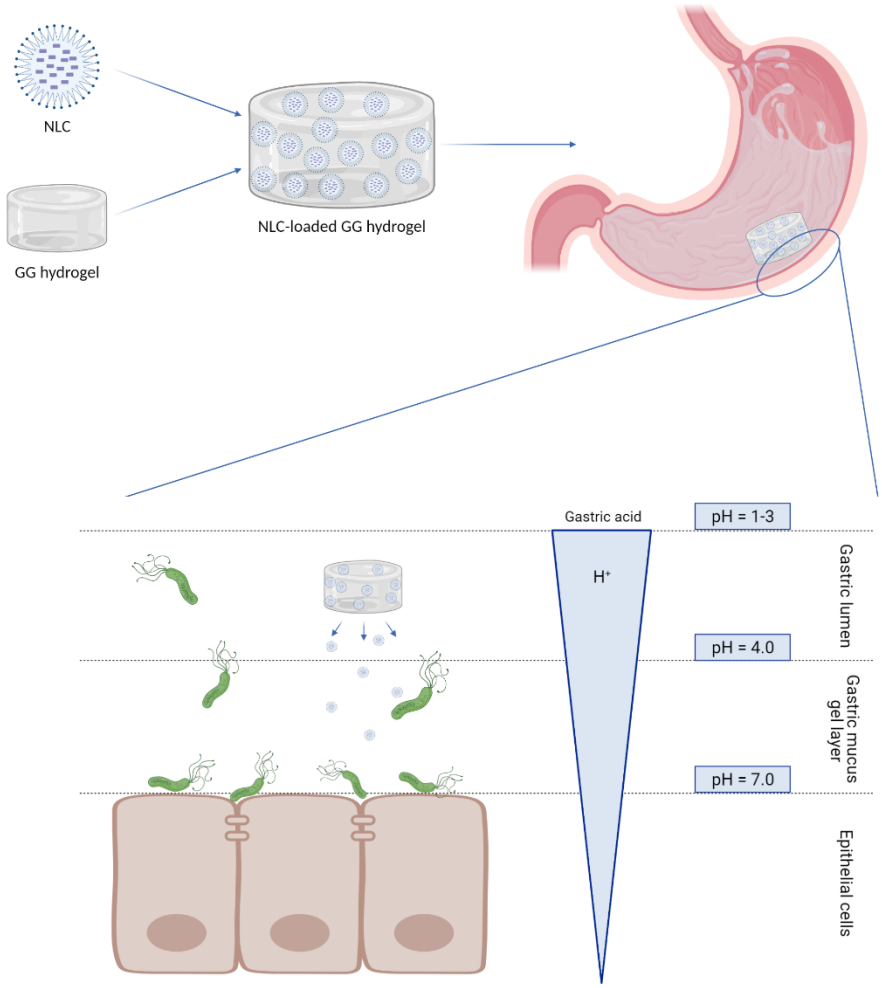


Figure 7. Schematic representation of the aim of the work. Image created with BioRender software.

Chapter II – Materials and Methods

2.1. NLC preparation and characterization

2.1.1. *NLC preparation*

NLC were prepared following a hot homogenization method adapted from Seabra *et al*. [56], as schematized in Figure 8. Briefly, 90 mg of the liquid lipid Miglyol-812® (Acofarma, Spain), 200 mg of the solid lipid Precirol® ATO5 (Gattefosé, France), and 60 mg of the surfactant Tween® 60 (Merck, Germany), were heated together at 65°C until melted and then blended with ultrapure water (Milli-Q® water; resistivity > 18 MΩ.cm, conductivity < 0.056 µS/cm and < 50 ppb of total organic carbons). The mixture was then sonicated for 5 min with an amplitude of 60% (Vibra-Cell model VCX 130 equipped with a VC 18 probe, Sonics and Materials Inc., Newtown, USA). The nanoparticles were stored at 4°C until further use and for a maximum period of 4 weeks.

For the later quantification assays, coumarin-6-loaded NLC (cNLC) were also prepared. For that, the same protocol was followed, except coumarin-6 (Sigma-Aldrich, USA) was mixed with Miglyol-812®. The final concentration of coumarin-6 used was 0.1% (w/v).

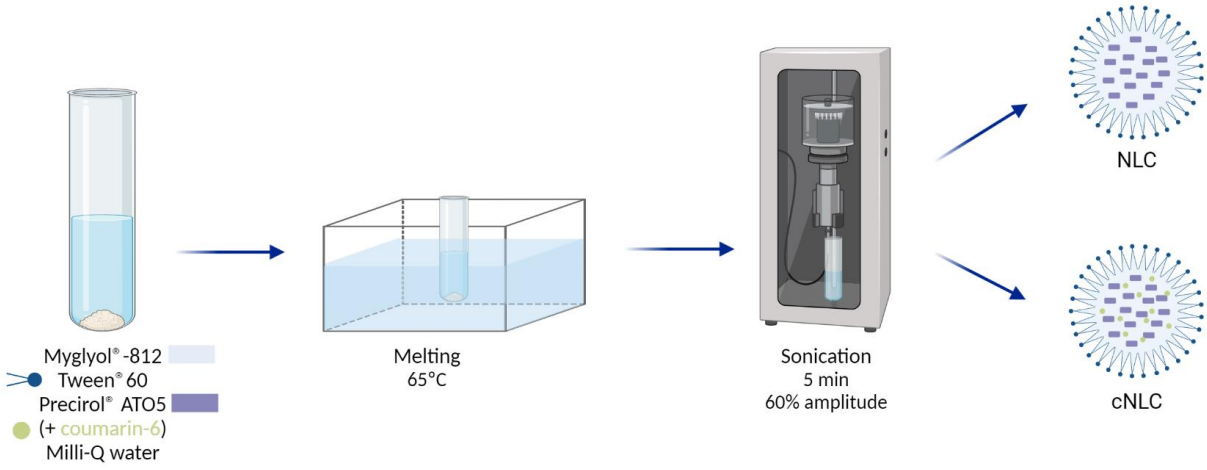


Figure 8. Schematic representation of NLC production by hot homogenization method. Image created with BioRender software.

2.1.2. Coumarin-6 encapsulation efficiency

To determine the encapsulation efficiency (EE) of coumarin-6 in cNLC, the nanoparticles were filtered using Amicon-4 filters of 50 kDa (Merck Millipore, USA) and centrifuged 15 min at 2500 revolutions per minute (rpm) using a Centrifuge 5810R (Eppendorf, Germany). The supernatant was collected to quantify the free coumarin-6 by fluorescent readings ($\lambda_{excitation}$ = 480 nm; $\lambda_{emission}$ = 560 nm) using a fluorimeter SynergyMx (BioTek, USA). The encapsulation efficiency was calculated using Eq. (1):

$$EE\ (\%) = \frac{C_I - C_{out}}{C_I}\ x\ 100 \qquad (1)$$

where C_I represents the total amount of coumarin-6 added during NLC preparation and C_{out} the total amount of coumarin-6 outside the NLC (i.e., in the supernatant).

2.1.3. *NLC characterization*

The size and surface charge (ζ-potential) of NLC were determined by dynamic light scattering (DLS) and electrophoretic light scattering (ELS), respectively, using a ZetaSizer Nano-ZS (Malvern Instruments, UK). Samples were prepared by diluting NLC in ultrapure water (Milli-Q®; 1:50) and were placed in a DTS1070 cuvette (Malvern Instruments, UK). Measurements were done in triplicate at 37°C, with a backscattering angle of 173°.

The NLC's concentration of each batch was measured by nanoparticle tracking analysis (NTA), at room temperature, using a NanoSight NS300 (Malvern Instruments, UK). Samples were prepared by diluting NLC in ultrapure water (Milli-Q®;1:200000).

2.2. GG hydrogels production and characterization

2.2.1. Hydrogels production

LAGG hydrogels were prepared by adapting the protocol of Silva-Correia *et al*. [129], as schematized in Figure 9. Briefly, LAGG powder (provided by I3Bs - Research Institute on Biomaterials, Biodegradables and Biomimetics of University of Minho) was dissolved in type I water (distilled water), at different concentrations (1.0, 1.5 and 2.0% (w/v)), under constant stirring. To completely dissolve the polymer and obtain a homogenous mixture, the solution was placed in a water bath, previously heated to 90°C, for 30 min. Afterwards, phosphate-buffered saline (PBS; 0.01M, pH 7.4), which worked as a crosslinker, was added under vigorous stirring, at a final concentration of 10% (v/v). This solution was then quickly transferred to a Petri dish (diameter 55 mm, Corning, France) and the gelation process occurred. The hydrogels were stored at 4°C in PBS overnight. Afterwards, small hydrogel discs were cut with a puncher of 9 mm diameter. Hydrogel's discs were stored immersed in PBS at 4°C until further use. LAGG hydrogels with NLC, with and without coumarin-6 (cNLC-LAGG and

NLC-LAGG, respectively), were also prepared. For that, the same protocol was followed and NLC were added at a final concentration of 10% (v/v) before the PBS addition step.

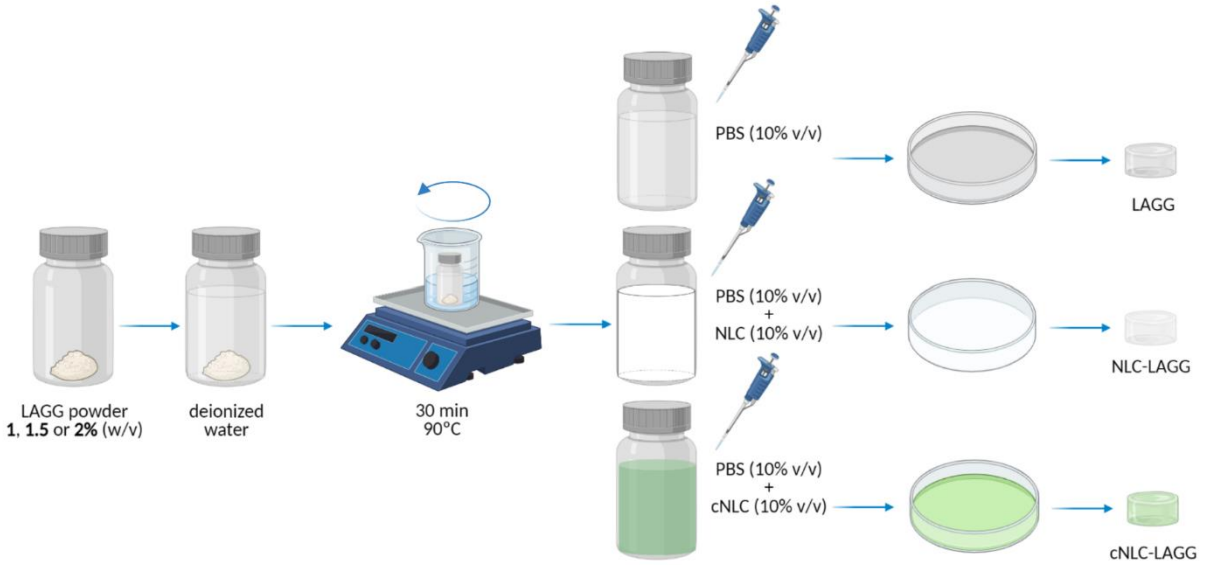


Figure 9. Schematic representation of LAGG hydrogels production. Image created with BioRender software.

HAGG hydrogels with a polymer concentration of 0.75% (w/v) were prepared using the same protocol previously described but without the addition of the crosslinking agent, PBS (Figure 10). Also, "mixed" hydrogels composed of LAGG (2% (w/v)) and HAGG (0.75% (w/v)) were prepared (HAGG:LAGG hydrogels) using the same protocol followed for HAGG. Different % ratios of HAGG and LAGG were tested: 75HAGG:25LAGG; 50HAGG:50LAGG; 25HAGG:75LAGG and 12.5HAGG:87.5LAGG. HAGG hydrogels and HAGG:LAGG hydrogels with NLC (NLC-HAGG and NLC-HAGG:LAGG, respectively), were also designed using a similar protocol, being NLC added at a final concentration of 10% (v/v) after the complete dissolution of the polymers' powder.

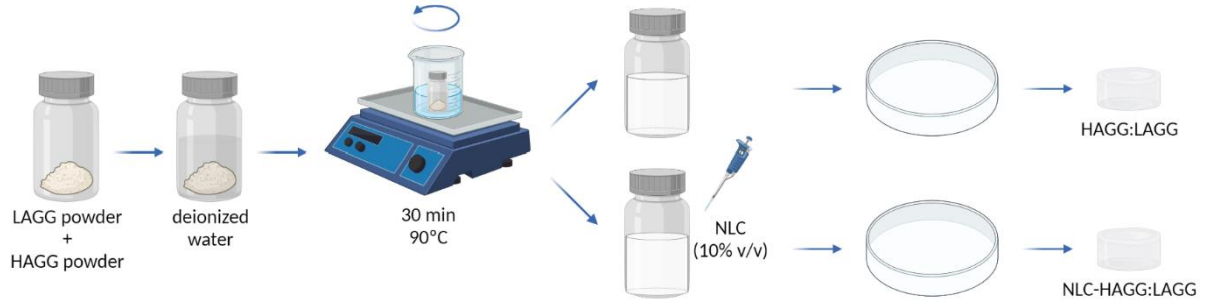


Figure 10. Schematic representation of HAGG and HAGG:LAGG hydrogels production. Image created with BioRender software.

2.2.2. Hydrogels' stability

LAGG, HAGG and HAGG:LAGG hydrogels' discs (with and without NLC) were placed in a 24-well plate (Falcon, USA) and immersed in 1 mL of buffers with distinct pH values: PBS pH 7.4; Sorensen's phosphate buffer (PB) pH 6.0; citrate-phosphate buffer (CB) pH 4.0; CB pH 2.0 and simulated gastric fluid (SGF), pH 1.2. Incubation proceeded under agitation (150 rpm), at 37°C, for 24 h. Weight and diameter of each hydrogel disc at each different pH condition was measured before (0 h) and after

incubation at different timepoints (2, 6 and 24 h for weight; 24 h for diameter). Weight variation was calculated using Eq. (2):

$$weight\ variation\ (\%) = \frac{W_t - W_0}{W_0}\ x\ 100 \quad (2)$$

where W_0 represents the weight before incubation and W_t the weight after each timepoint. Diameter variation was calculated using Eq. (3):

$$diameter\ variation\ \ (\%) = \frac{D - D_0}{D_0}\ x\ 100 \quad (3)$$

where D_0 represents the diameter before incubation and D the diameter after 24h incubation.

2.2.3. Hydrogels' mechanical behavior

The mechanical behavior of LAGG, HAGG and HAGG:LAGG hydrogels' discs, both with and without NLC, was tested by dynamic mechanical analysis (DMA), conducted over 30 min at 37°C and using a TRITEC 2000 (TRITON Technology, UK). Samples were compressed with a displacement corresponding to 1 % of the hydrogels height and a single frequency of 0.05Hz to simulate the contractile forces of the stomach (about three contractions per minute) [130]. Figure 11 schematizes the parameters obtained by DMA analysis.

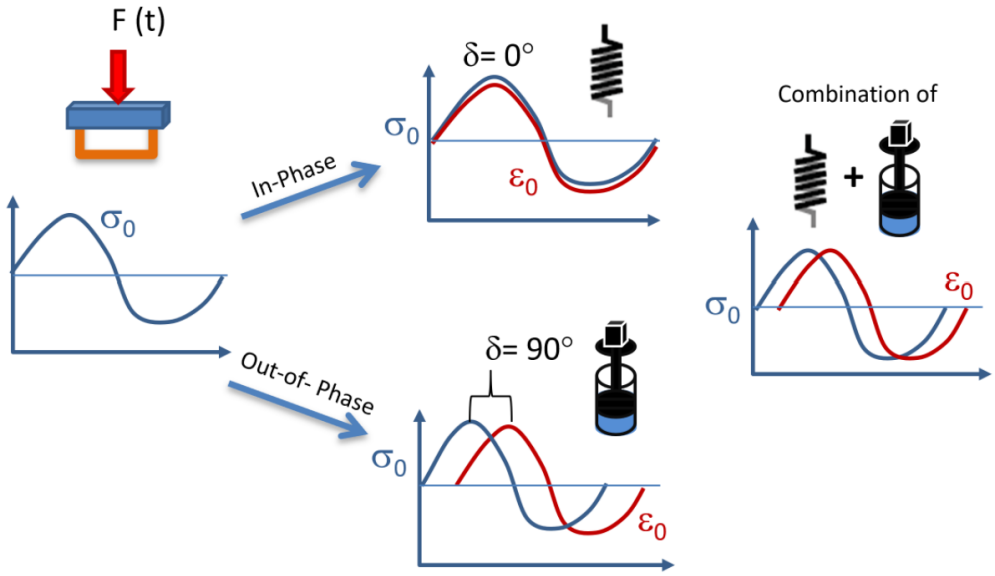


Figure 11. Responses measured by DMA technique after stress application. From DMA analysis, it is possible to extract three main values: (1) storage modulus (or elastic modulus), that corresponds to the in-phase response of the material and is a measure of its ability to store energy; (2) loss modulus (or viscous modulus), that corresponds to the out-of-phase response and is related to the damping behavior of the material which is its ability to dissipate energy; and (3) tan δ, the ratio between loss modulus and storage modulus [131]. For Hookean solids, the response is completely in-phase with the applied stress (δ=0°), while for Newtonian liquids is completely out-of-phase (δ=90°). Viscoelastic materials present an intermediate behavior. Blue line (σ) – stress; red line (ε) – strain (response of the material). From Polymer Properties Database [132].

2.2.4. NLC distribution in the hydrogels

Confocal microscopy was used to analyze cNLC distribution in cNLC-LAGG hydrogels' discs. Images were acquired with a TCS SP5II confocal microscope (Leica, Germany) with a 63x objective. The software Image J was used to treat the images.

2.3. NLC release from GG hydrogels

2.3.1. Quantification by fluorescence analysis

cNLC-LAGG hydrogels' discs were placed in a 24-well plate (Falcon, USA) and immersed in 1mL of different buffers: PBS pH 7.4; PB pH 6.0; CB pH 4.0; CB pH 2.0 and SGF pH 1.2. Then, incubation was done under agitation (150 rpm) at 37°C, for 24 h. 50 µL of the supernatant at each pH condition were collected before (0 h) and after incubation at different timepoints (1, 2, 3, 6 and 24 h). The concentration of released cNLC was determined by fluorescence analysis using a fluorimeter SynergyMx (Biotek, USA), with an excitation peak at a wavelength of 420 nm and an emission peak at 490 nm. To convert the fluorescence values in cNLC concentration, a calibration curve was previously done. For that, solutions with known concentration of cNLC were made in each buffer, the fluorescence was measured, and the calibration curve was obtained.

2.3.2. Quantification by NTA

NLC-LAGG, NLC-HAGG and NLC-HAGG:LAGG hydrogels' discs were placed in a 24-well plate (Falcon, USA), immersed in 1 mL of buffers with different pH as in section 2.3.1 and incubated under agitation (150 rpm) at 37°C. At different timepoints, the supernatants were collected (Table 5) and the concentration of released nanoparticles was determined by NTA using a NanoSight NS300 (Malvern Instruments, UK).

Table 5. Timepoints used for NLC quantification by NTA.

Type of hydrogels	Timepoints
LAGG	24, 48 and 72 h
HAGG and HAGG:LAGG	2, 6 and 24 h

2.4. Antimicrobial testing

2.4.1. H. pylori culture conditions

Human isolated *H. pylori* J99 strain (provided by Department of Medical Biochemistry and Biophysics, Umeã University, Sweden) was first cultured in spots in *H. pylori* solid medium at 37ºC, under microaerophilic settings (5% O_2, 15% CO_2, 80% N_2, bioMérieux SA, France). After 48 h, some

colonies were streaked in *H. pylori* solid medium and incubated for another 48 h, under the same conditions. The *H. pylori* solid medium was composed of blood agar base 2 (Oxoid, France) supplemented with 10% (v/v) defibrinated horse blood (Probiológica, Portugal) and with 0.2% (v/v) antibiotics-cocktail of 0.155 g/L Polymixin B, 6.25 g/L Vancomycin, 1.25 g/L Amphotericin B and 3.125 g/L Trimethoprim (all from Sigma-Aldrich, USA).

Then, to assure bacteria were in their fittest condition prior to testing, an *H. pylori* pre-inoculum was done. For that, *H. pylori* was removed from the solid medium by streaking 1 mL of PBS with a T-spreader on the medium surface. Afterwards, the liquid was collected and centrifuged for 5 min at 3600 *g*. The pellet, containing the bacteria, was then resuspended in *H. pylori* liquid medium (Brucella Broth medium (BB, Oxoid, France) supplemented with 10% (v/v) of heat inactivated Fetal Bovine Serum (FBS, Gibco, USA)). Finally, the bacteria were transferred to a T25-flask (SPL Life Sciences, Korea) and adjusted to an optical density (OD) of 0.1 (λ= 600 nm; UV/VIS spectrophotometer Lambda 45, Perkin Elmer, USA) in *H. pylori* liquid medium [56]. Incubation proceeded overnight in a microaerophilic environment, under agitation (150 rpm), at 37°C.

2.4.2. Effect of GG hydrogels and their extracts on H. pylori growth

H. pylori J99 at a concentration of approximately $1x10^7$ colony forming unit (CFU)/mL [41], were incubated with either LAGG or NLC-LAGG hydrogels' discs, for 24h, at 37°C, with 150 rpm agitation in 600 µL of BB+10%FBS medium and under microaerophilic conditions. After, 20 µL of each culture were collected, serially diluted in PBS (until 1:100000) and plated on *H. pylori* solid medium plates. After 3 to 5 days of incubation, at 37°C under microaerophilic conditions, the number of viable bacteria was determined by CFU counting.

The antimicrobial activity of LAGG hydrogels' extracts was also evaluated. For that, LAGG and NLC-LAGG hydrogels were incubated over different timepoints (24, 48 and 72 h), in pH 7.4 and pH 2.6, at 37ºC and under agitation (150 rpm). After, the supernatants were collected (i.e., the extracts of the hydrogels) and these were incubated for 24 h in 100 µL of BB+10% FBS medium, at 37°C, 150 rpm, under microaerophilic conditions. The same protocol used for LAGG hydrogels was followed to determine the number of viable cells after exposure to the extracts.

2.5. Statistical analysis

Statistical analysis was performed with Graph Pad Prism v 8.0 (Graph-Pad Software, La Jolla, USA). Results are presented as the mean ± the standard deviation. Statistical significance was determined using a t-test or a two-way ANOVA test as adequate. Values of $p<0.05$ were considered statistically significant.

Chapter III – Results

3.1. NLC preparation and characterization

The NLC protocol used was an adaptation of the original protocol described by Seabra *et al*. [56], as schematized in Figure 8. Both NLC and cNLC were successfully produced as demonstrated by their characterization.

The obtained nanoparticles were characterized by three different techniques and results are shown in Figure 12. First, dynamic light scattering (DLS) was used to evaluate the size of the nanoparticles in suspension. The mean diameter of NLC was 302.0±17.4 nm, while cNLC presented a diameter of 314.1±19.5 nm. The polydispersity index (PI) was circa 0.3 for both NLC and cNLC. The surface charge of the nanoparticles, ζ-potential, was obtained by electrophoretic light scattering (ELS). NLC and cNLC presented a surface charge of -27.43±2.98 mV and -28.73±2.01 mV, respectively. Finally, the concentration was evaluated by nanoparticle tracking analysis (NTA). The average NLC concentration was $1.01x10^{13}$±$6.34x10^{12}$ nanoparticles/mL and $8.46x10^{12}$±$6.77x10^{12}$ nanoparticles/mL for cNLC. No significant differences were observed in all parameters between NLC and cNLC.

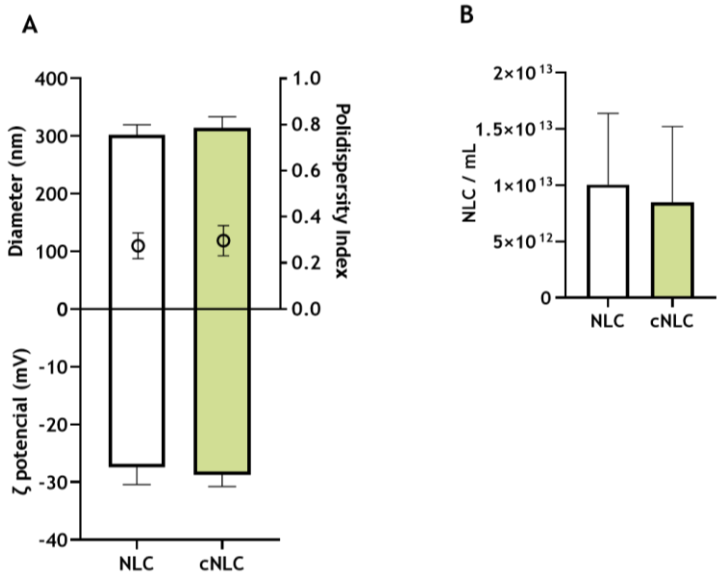


Figure 12. NLC characterization. (A) Size (upper bars), polydispersity index (PI, dots) and surface charge (lower bars); (B) Concentration. Size and PI were obtained by DLS, ζ-potential was obtained by ELS and concentration was obtained by NTA (n=18 for NLC; n=12 for cNLC).

Regarding cNLC, the encapsulation efficiency of coumarin-6 was also determined. For that, the nanoparticles were filtered using an Amicon-4 filter of 50 kDa that does not allow the passage of cNLC but that free coumarin-6 is able to cross. The supernatant was collected for fluorescence readings ($\lambda_{excitation}$ = 480 nm; $\lambda_{emission}$ = 560 nm) and fluorescence was converted in coumarin-6 concentration using the previously determined calibration curve of free coumarin-6 in water (Figure 13).

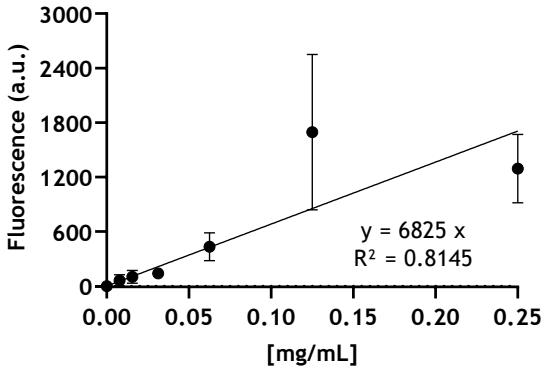


Figure 13. Coumarin-6 calibration curve in water. $\lambda_{excitation}$ = 480 nm; $\lambda_{emission}$ = 560 nm.

The encapsulation efficiency of coumarin-6 in NLC was set at 96.4%.

3.2. LAGG hydrogels production and characterization

3.2.1. LAGG hydrogels production

LAGG hydrogels were produced by adapting the protocol described by Silva-Correia *et al*. [129], as schematized in Figure 9. LAGG hydrogels with polymer concentration of 1% w/v (LAGG 1%), 1.5% w/v (LAGG 1.5%) and 2% w/v (LAGG 2%) were successfully produced. However, LAGG 1% did not present mechanical properties to allow its handling and did not undergo further experiments. As such, only LAGG 1.5% and LAGG 2% hydrogels were used in further tests.

NLC were incorporated on the hydrogels (NLC-LAGG) at a concentration of 10% w/v, following the same protocol. cNLC were also incorporated in the hydrogels (cNLC-LAGG). Both NLC-LAGG and cNLC-LAGG hydrogels were successfully produced with polymer concentrations of 1.5% and 2% w/v. The obtained hydrogels are presented in Figure 14.

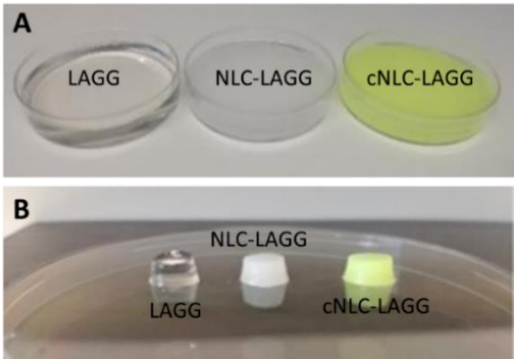


Figure 14. LAGG, NLC-LAGG and cNLC-LAGG hydrogels. (A) hydrogels after production and (B) after being cut with a 9 mm puncher.

3.2.2. LAGG hydrogels' stability

The hydrogels' stability was accessed by monitoring diameter and weight changes over incubation periods at different pH conditions (to mimic the gastric environment more closely). The diameter (Figure 15) and weight (Figure 16) of LAGG (2% & 1.5%) and NLC-LAGG (2% & 1.5%) hydrogels' discs were measured before and after incubation in a pH range from 1.2 to 7.4 and for a maximum period of 24 h.

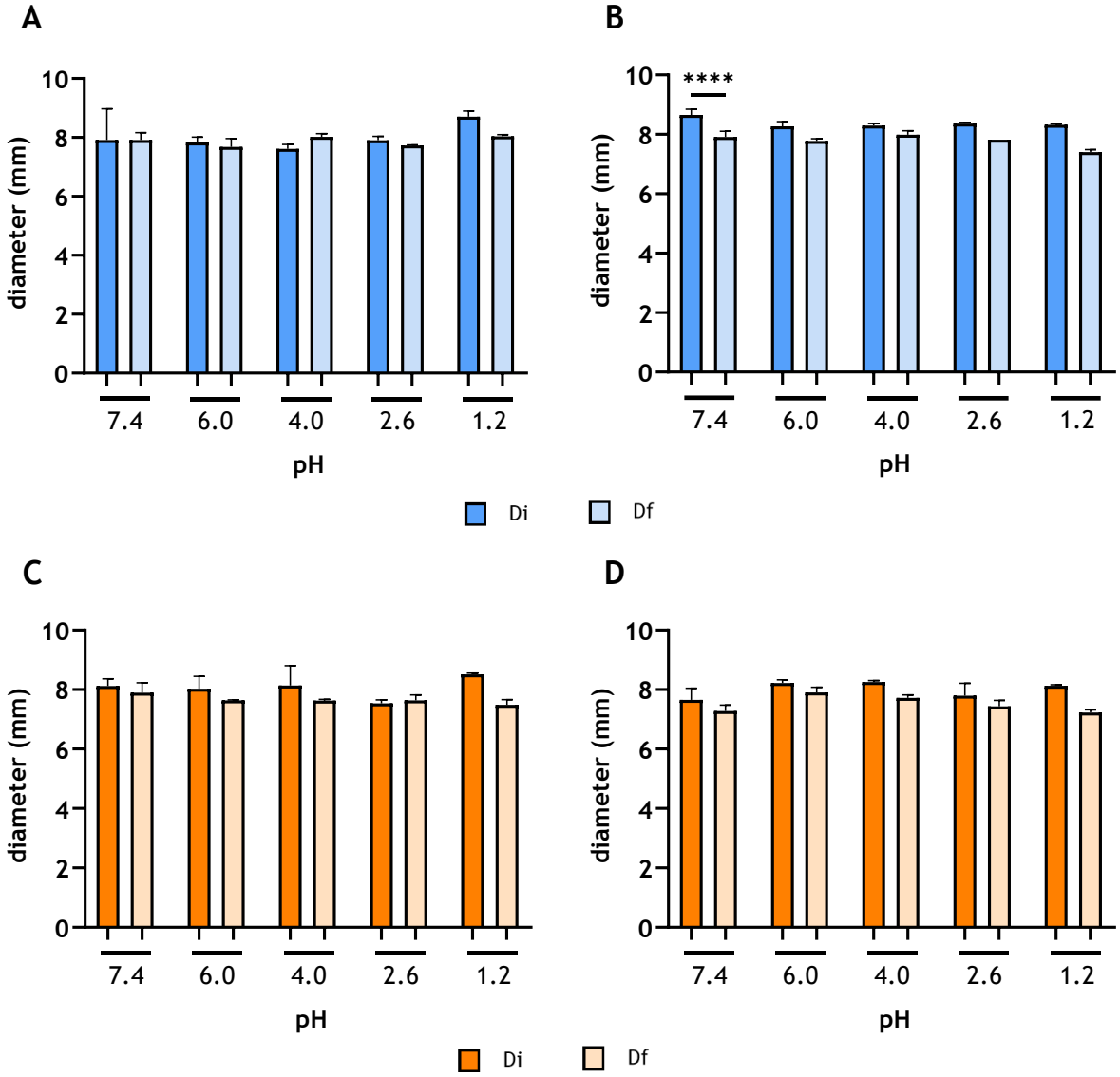


Figure 15. LAGG hydrogels' diameter. (A) LAGG 2%; (B) LAGG 1.5%; (C) NLC-LAGG 2%; (D) NLC-LAGG 1.5%. Hydrogels' discs were incubated in different pH conditions, for 24 h, at 37°C, under agitation (150 rpm). Diameter was measured with a digital paquimeter before (Di) and after (Df) incubation (t test; **** - significantly different from each other, $p<0.0001$; n=2).

After 24 h, the hydrogels' diameter didn't suffer significant changes (Figure 15 A and B), being a similar behavior observed for NLC loaded hydrogels (Figure 15 C and D). Even though there were no variations on the hydrogel's diameter, weight reduction was observed for all the hydrogels tested, in all pH conditions and for every timepoint (Figure 16).

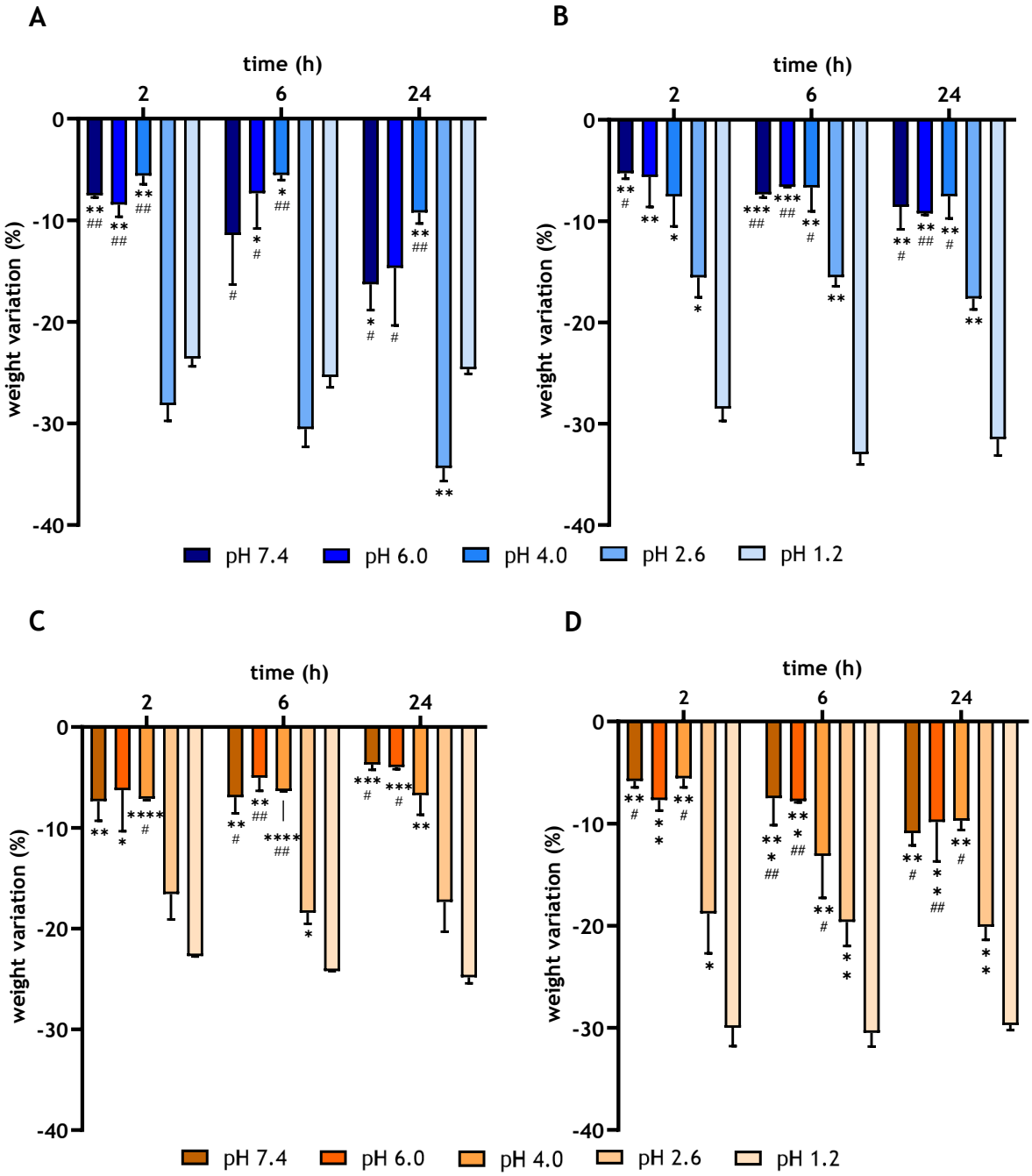


Figure 16. Stability of LAGG hydrogels in different mediums. (A) LAGG 2%; (B) LAGG 1.5%; (C) NLC-LAGG 2%; (D) NLC-LAGG 1.5%. Hydrogels were incubated in different pH for 24 h, at 37°C, under agitation (150 rpm). Hydrogels' weight was measured before and after incubation (t test; *,**,***,**** - significantly different weight variation from pH 1.2, $p<0.05$, $p<0.01$, $p<0.001$, $p<0.0001$, respectively; #, ##, ###, #### - significantly different weight variation from pH 2.6, $p<0.05$, $p<0.01$, $p<0.001$, $p<0.0001$, respectively; n=2).

Regarding time, higher mass loss occurred over the first two hours (more pronounced weight variation), followed by a stabilization of the weight up to 24 h. Regarding weight variations according to the pH conditions tested, it was observed higher mass loss in more acidic mediums, specifically in pH 2.6 and pH 1.2. No significant differences were observed between the other three pH conditions tested (pH 7.4, 6.0 and 4.0). These results showed that LAGG hydrogels are mainly influenced by more acidic pHs and during the first 2 h of incubation. Comparing LAGG 2% (Figure 16A) and LAGG 1.5%

(Figure 16B), i.e., hydrogels with different polymer concentration, differences were only observed at pH 1.2, having the LAGG 1.5% hydrogels higher weight variation (higher mass loss). Finally, the addition of NLC to either LAGG 2% or LAGG 1.5% did not affect the overall stability of the hydrogels, as similar results were obtained comparing to the "bare" hydrogels (no NLC addition) (Figure 16 C and D).

3.2.3. LAGG hydrogels' mechanical behavior

The mechanical properties of both LAGG (2% & 1.5%) and NLC-LAGG (2% & 1.5%) hydrogels' discs were accessed by DMA. For that, a compression test was performed for 30 minutes. The obtained results are presented in Figure 17.

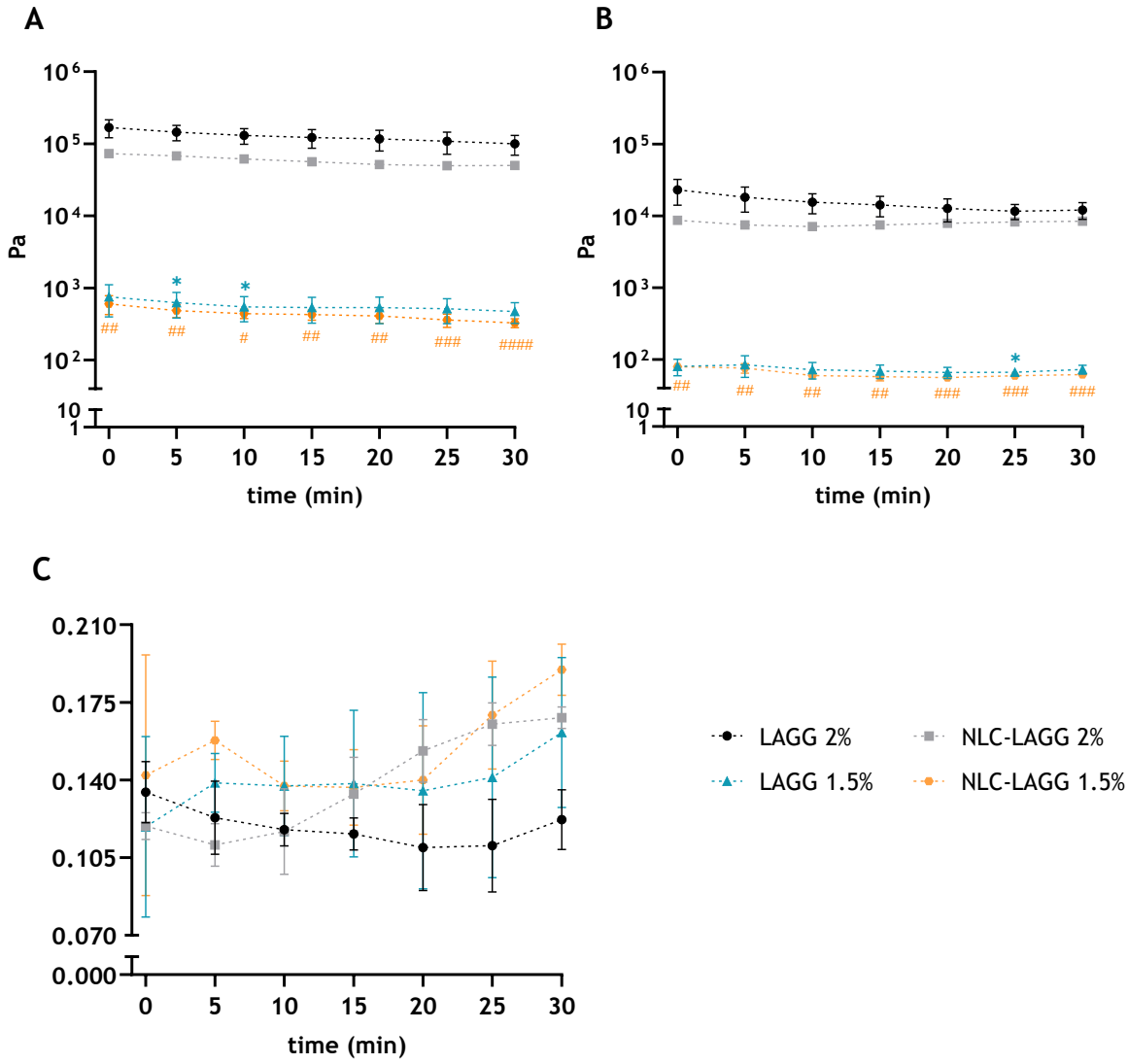


Figure 17. Mechanical behavior of LAGG hydrogels. (A) storage modulus, (B) loss modulus and (C) tan δ were accessed by DMA, compressing both LAGG (2% & 1.5%) and NLC-LAGG (2% & 1.5%) hydrogels with a frequency of 0.05 Hz and a displacement of 0.04 ± 0.01 mm, for 30 min, at 37°C (two-way ANOVA; * - significantly different from LAGG 2%, $p<0.05$; #, ##, ###, #### - significantly different from LAGG 1.5%, $p<0.05$, $p<0.01$, $p<0.001$, $p<0.0001$, respectively; n=3).

Both storage (Figure 17A) and loss moduli (Figure 17B) remained stable during the compression test. Also, the addition of NLC to the designed hydrogels did not affect their mechanical properties since no significant differences were observed for both moduli between LAGG and NLC-LAGG hydrogels at both concentrations tested (Figure 17 A and B). On the other hand, polymer concentration affected the ability of the hydrogels to both store and dissipate energy. The hydrogels with higher LAGG concentration (2% w/v) presented higher moduli than the LAGG 1.5% ones.

All tested hydrogels presented a higher storage modulus than loss modulus throughout the 30 minutes (tan δ <1) (Figure 17C). These low tan δ values are characteristic of elastic behavior.

3.2.4. NLC distribution in LAGG hydrogels

To evaluate the nanoparticles distribution and incorporation on the hydrogels' structure, hydrogels' discs with coumarin-6 loaded NLC (cNLC-LAGG) were observed under confocal microscopy, due to the fluorescence properties of coumarin-6. Figure 18 represents a 3D projection of multiple images obtained from different stacks of the sample. The green dots correspond to the fluorescent cNLC present within the structure of the hydrogel.

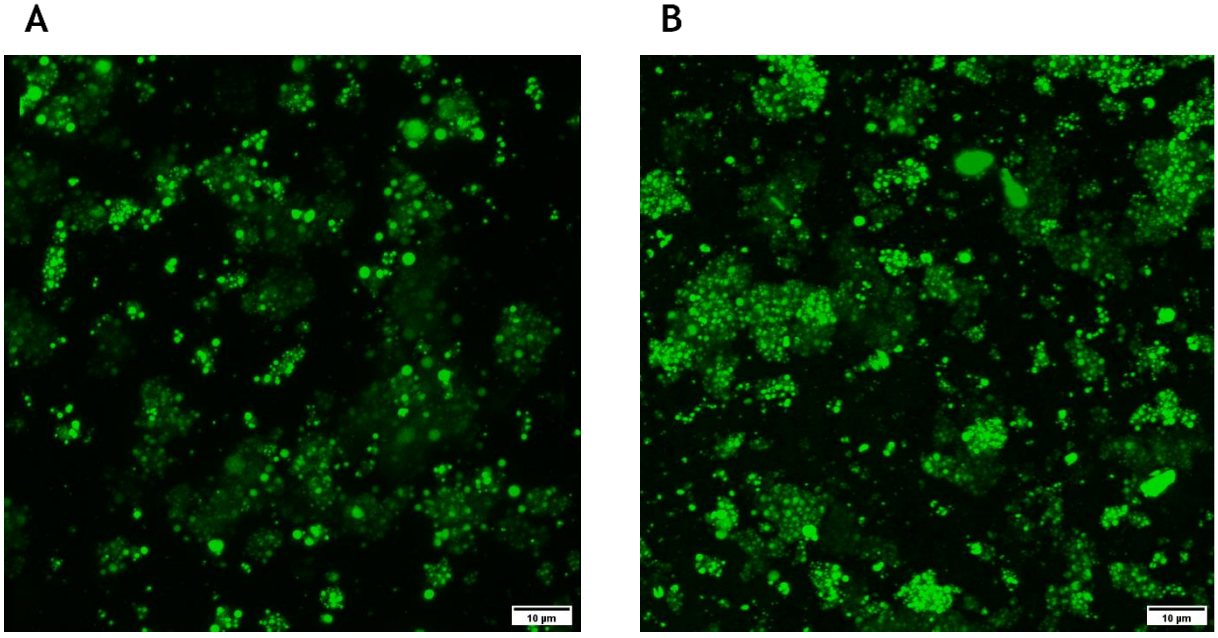


Figure 18. NLC distribution in LAGG hydrogels. (A) cNLC-LAGG 2%; (B) cNLC-LAGG 1.5%. Images of cNLC-LAGG hydrogels' discs were obtained by confocal microscopy using a 63x (oil) objective and were treated with ImageJ software. Scale bar: 10 µm.

The obtained images confirmed that the nanoparticles were evenly distributed throughout both cNLC-LAGG 2% (Figure 17A) and cNLC-LAGG 1.5% (Figure 17B) hydrogels.

3.3. NLC release from LAGG hydrogels

The release profile of NLC from LAGG hydrogels was evaluated by two different methods: fluorescence analysis and nanoparticle tracking analysis. The theoretical quantity of NLC in each hydrogel's disc, calculated by correlating the disc's volume with the NLC's concentration, is given in Table 6.

Table 6. Absolute number of NLC in each LAGG hydrogel's disc.

NLC-LAGG 2%	NLC-LAGG 1.5%
$1.50x10^{11} \pm 2.24x10^{10}$	$1.52x10^{11} \pm 1.19x10^{10}$

3.3.1. Fluorescence analysis

Due to its fluorescent properties, coumarin-6 can be easily detected by a fluorimeter. Therefore, cNLC-LAGG (2% & 1.5%) hydrogels were used to quantify the nanoparticles release in different pH conditions through fluorescence analysis. First, the emission spectrum of cNLC was obtained to understand if the components of the nanoparticles could influence the fluorescence emission of coumarin-6.

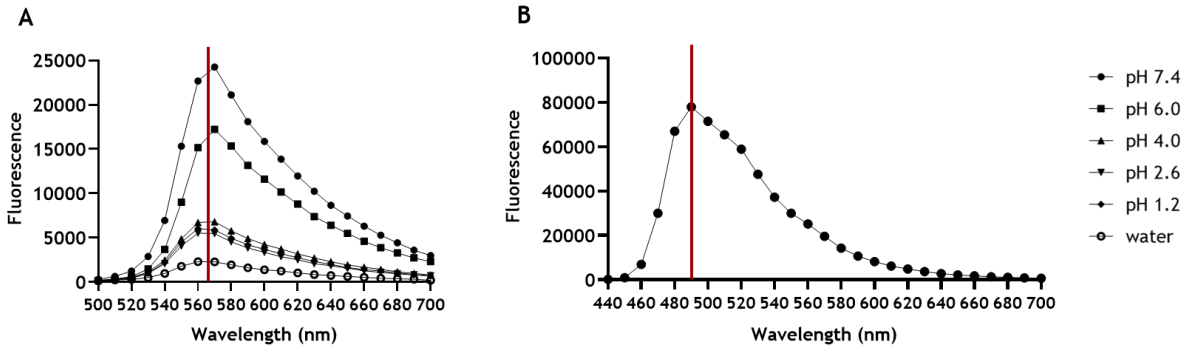


Figure 19. Emission spectrums of free coumarin-6 and coumarin-6-loaded NLC (cNLC). (A) Emission spectrum of coumarin-6 with an excitation wavelength of 480 nm; (B) Emission spectrum of cNLC with an excitation wavelength of 420 nm.

In fact, it was observed a shift in the emission peak from around 460 nm when using free coumarin-6 to 490 nm when using the cNLC (Figure 19). As such, the emission wavelength selected for further release quantification protocol was 490 nm.

The supernatants of the hydrogels' discs were collected at different timepoints after incubation in mediums with different pH for quantification of the released cNLC. Fluorescence was measured ($\lambda_{excitation}$ = 420 nm; $\lambda_{emission}$ = 490 nm) and converted in cNLC concentration using the respective calibration curve for each pH setting (Figure 20).

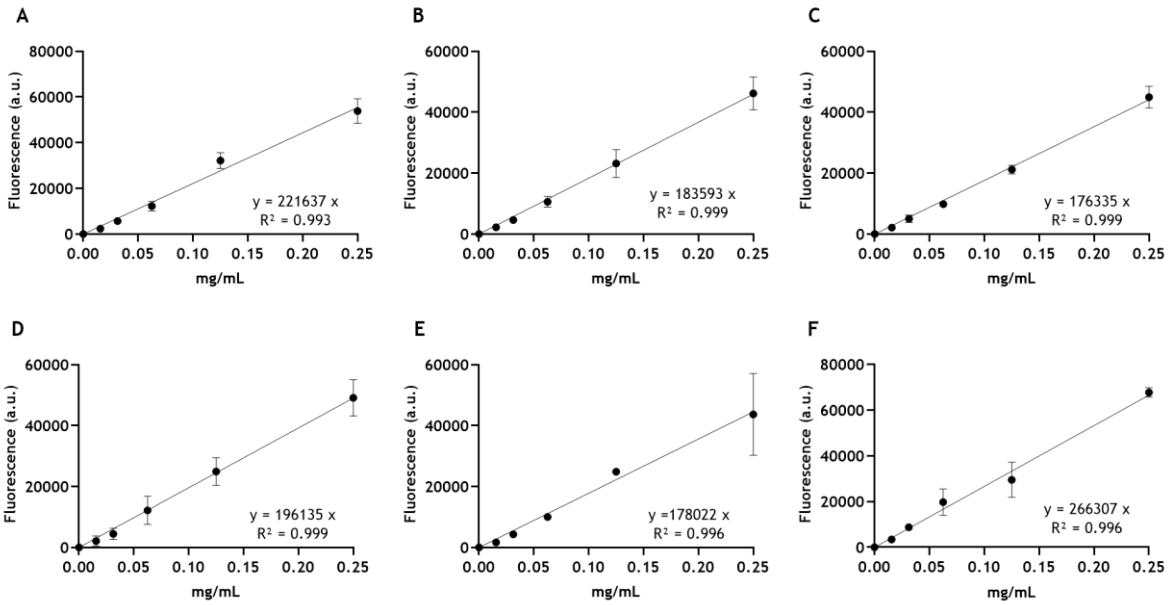


Figure 20. cNLC calibration curves in different pH conditions (different mediums). (A) pH 7.4; (B) pH 6.0; (C) pH 4.0; (D) pH 2.6; (E) pH 1.2; (F) water. $\lambda_{excitation}$ = 420 nm; $\lambda_{emission}$ = 490 nm.

The percentage of nanoparticles released from cNLC-LAGG 2% and cNLC-LAGG 1.5% hydrogels is shown in Figure 21.

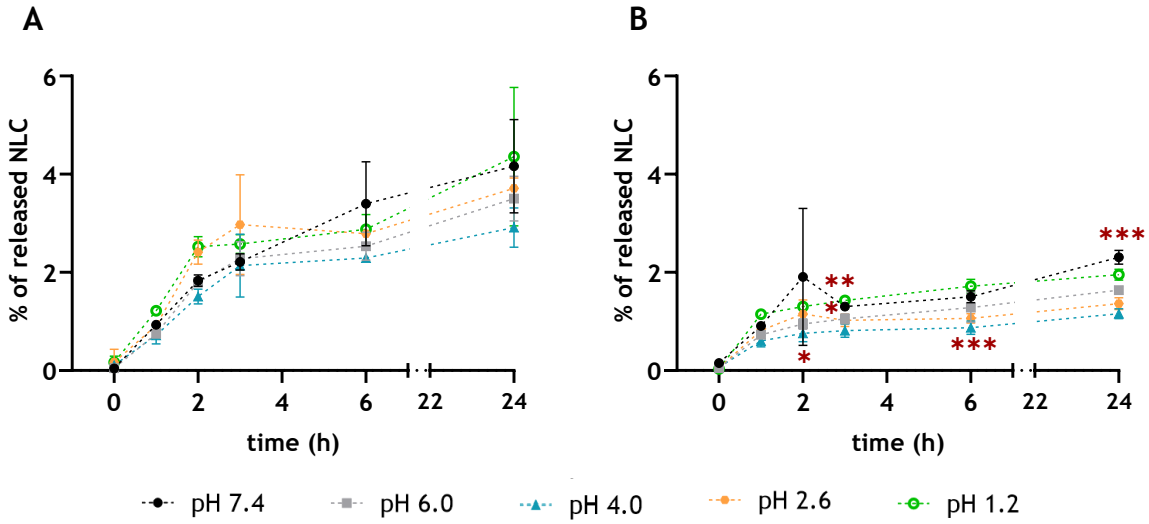


Figure 21. cNLC release from LAGG hydrogels in different mediums. (A) cNLC-LAGG 2% and (B) cNLC-LAGG 1.5%. Hydrogels' discs were incubated in different pH for 24 h, at 37°C, under agitation (150 rpm). Supernatants were collected for fluorescent readings: $\lambda_{excitation}$ = 420 nm and $\lambda_{emission}$ = 490 nm (t test; *, *** – significantly different from cNLC-LAGG 2%, p<0.05, p<0.001, respectively; n=3).

The obtained results indicate that LAGG hydrogels can release the NLC (Figure 21). However, cNLC-LAGG 2% (Figure 21A) were able to release more nanoparticles than cNLC-LAGG 1.5% (Figure 21B), as shown by the average number of released cNLC after 24 h of incubation (Table 7).

Table 7. Number of cNLC released from LAGG hydrogels in different pH conditions. The number of nanoparticles that were release from cNLC-LAGG hydrogels' discs was quantified by fluorescence analysis after 24 h of incubation.

pH	cNLC-LAGG 2%	cNLC-LAGG 1.5%
7.4	$6.04x10^9$	$3.47x10^9$
6.0	$4.86x10^9$	$2.35x10^9$
4.0	$4.19x10^9$	$1.97x10^9$
2.6	$5.11x10^9$	$2.10x10^9$
1.2	$5.80x10^9$	$2.73x10^9$

For cNLC-LAGG 2% hydrogels' discs, the pH did not affect the cNLC release profile (Figure 21A). However, for the less concentrated hydrogels (Figure 21B), the pH had an effect on the nanoparticles release, with higher cNLC being released at pH 7.4 and pH 1.2 (the extremes on the pH range tested).

3.3.2. Nanoparticle tracking analysis

Another method that was used to quantify NLC release from the designed hydrogels was NTA, which also allows the visualization of the nanoparticles.

NLC-LAGG (2% & 1.5%) hydrogels' discs were incubated in pH 7.4 and pH 2.6 for 72 h and supernatants were collected at different timepoints (24, 48 and 72 h). The percentage of nanoparticles that were released from the hydrogels are presented in Figure 22.

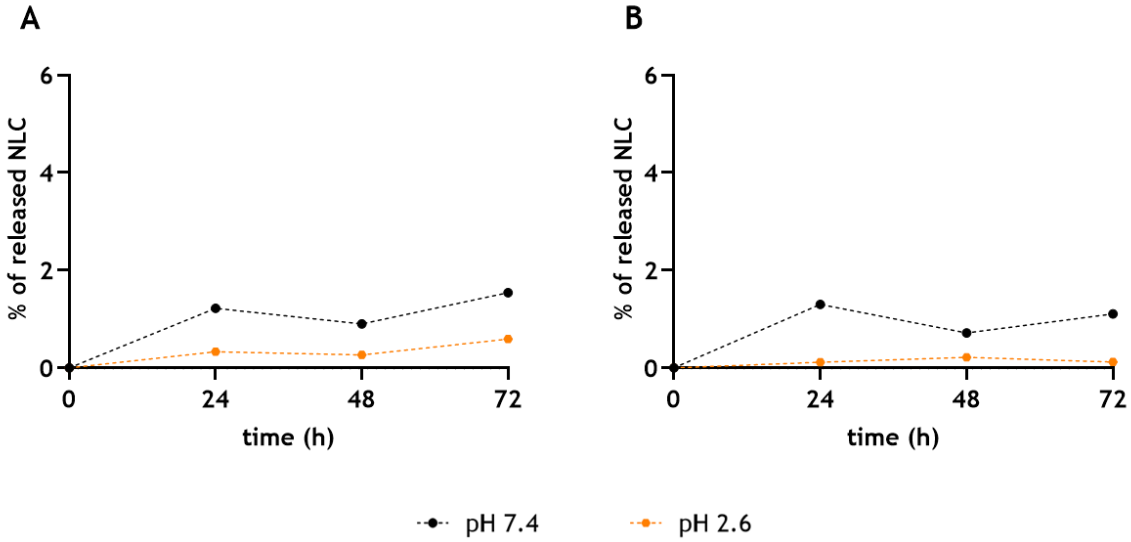


Figure 22. NLC release from LAGG hydrogels in different mediums. (A) NLC-LAGG 2% and (B) NLC-LAGG 1.5%. Hydrogels' discs were incubated in different pH, at 37°C, under agitation (150 rpm). Supernatants were collected and analyzed with NTA technique (n=2).

Results indicate slightly higher NLC release at pH 7.4 than at pH 2.6. However, the percentage of nanoparticles released was very low (less than 2%) at both pH and for both NLC-LAGG 2% and 1.5% hydrogels' discs. When comparing the number of NLC released after 24 h of incubation obtained by fluorescence analysis (Table 7) with the ones obtained by NTA (Table 8), it is possible to observe that a lower number was obtained when using the NTA technique, particularly at pH 2.6.

Table 8. Number of NLC released from LAGG hydrogels in different pH conditions. The number of nanoparticles that were release from NLC-LAGG hydrogels' discs was quantified by NTA after different timepoints (24, 48 and 72 h).

pH	Time of incubation (h)	NLC-LAGG 2%	NLC-LAGG 1.5%
7.4	24	$2.30x10^9$	$2.49x10^9$
	48	$1.70x10^9$	$1.38x10^9$
	72	$2.90x10^9$	$2.12x10^9$
2.6	24	$5.32x10^8$	$1.76x10^8$
	48	$4.35x10^8$	$3.23x10^8$
	72	$9.63x10^8$	$1.79x10^8$

The collected supernatants were used to access the antimicrobial activity of NLC-LAGG hydrogels' extracts against *H. pylori* J99, which is described on the next subsections.

3.4. Antimicrobial properties of LAGG hydrogels

First, to exclude any possible interference of the polymer on *H. pylori* viability, the antimicrobial activity of LAGG hydrogels was tested. For that, LAGG 2% hydrogels' discs, with and without nanoparticles, were incubated directly with a suspension of *H. pylori* over 24 h. Afterwards, the supernatant was collected, and bacterial cell viability was assessed by CFU counting. Results are presented in Figure 23.

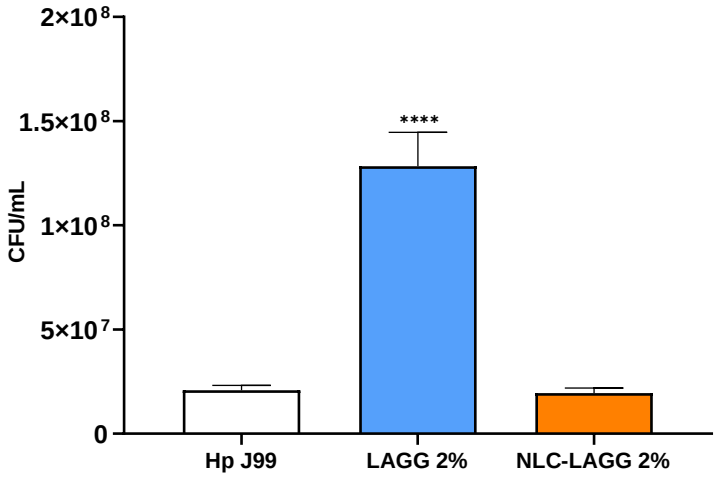


Figure 23. Antimicrobial activity of LAGG and NLC-LAGG hydrogels. LAGG 2% and NLC-LAGG 2% hydrogel's discs were incubated with *H. pylori* J99 (Hp J99) for 24h. The number of viable bacteria was determined by CFU counting. A pure culture of *H. pylori* J99 was used as positive control (t test; **** - significantly different from the control, $p<0.0001$; n=2 with triplicates).

The bare LAGG 2% hydrogels' discs (without NLC) did not have antimicrobial effect, since after 24 h of incubation no reduction in the number of viable cells when comparing to the control was observed (Figure 22). Therefore, if any reduction on the bacterial load would be observed, it would only be related to the NLC released from the hydrogel. Also, when incubating the NLC-LAGG 2% hydrogels with *H. pylori* J99, no significant decrease in the number of CFUs were seen compared to the pure

culture, which indicates that the amount of NLC released after 24 h in these experimental conditions was not sufficient to have an antibacterial effect, either bactericidal or bacteriostatic.

Therefore, to evaluate if an extended incubation time (over 24 h) or different pH settings could impact or even improve the NLC release and consequently, the overall antibacterial performance, subsequent antibacterial tests were performed using the hydrogel discs' extracts. For that, LAGG and NLC-LAGG (2% & 1.5%) hydrogel's discs were pre-incubated for a maximum period of 72 h, with supernatants being collected at different timepoints. Afterwards, these supernatants were incubated with *H. pylori* J99 for 24 h and then the number of viable bacteria was determined by CFU counting. Results are presented in Figure 24.

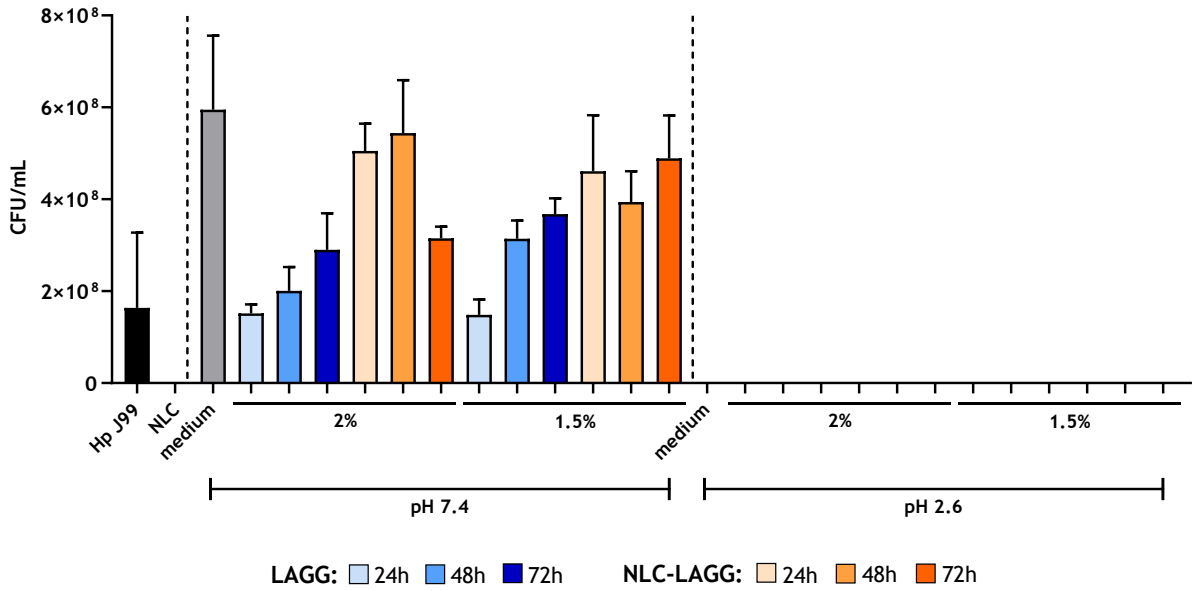


Figure 24. Antimicrobial activity of the extracts of LAGG hydrogels. LAGG (2% & 1.5%) and NLC-LAGG (2% & 1.5%). Hydrogel's discs were incubated in pH 7.4 and pH 2.6 for 72 h. *H. pylori* J99 pure culture was used as positive/growth control. For the negative control, *H. pylori* J99 was incubated with NLC in a bactericidal concentration (10^{12} NLC/mL). To access the effect of the pH per se on bacteria, *H. pylori* J99 was incubated with both buffers at pH 7.4 and pH 2.6 (n=2 with triplicates).

As expected, after incubation with a bactericidal concentration of NLC (10^{12} NLC/mL, 2nd bar) [133], no viable bacteria were detected.

Regarding the extracts of the hydrogel's discs incubated at pH 7.4 (4th to 15th bars), no antimicrobial activity was observed. On the other hand, bacteria did not remain viable when incubated with the extracts of the hydrogels incubated at pH 2.6 (17th to 28th bars). However, the antimicrobial effect observed was due to the medium pH and not to NLC present in the extracts, since no viable bacteria were detected on the growth control at pH 2.6 (16th bar). This occurred because although *H. pylori* can survive in harsh gastric conditions, the medium with pH 2.6 was a buffer and, therefore, bacteria were unable to use its urease activity and buffer it to a more neutral pH. These preliminary results indicate that the number of NLC released, even after 72 h of incubation and in different pH settings, were not enough to achieve bactericidal levels and, therefore, decrease the bacterial load.

3.5. Hydrogel optimization to improve NLC release

With the aim to improve NLC release, other combinations of polymers with LAGG were designed.

3.5.1. HAGG:LAGG hydrogels production

High acyl gellan gum (HAGG) hydrogels were produced by adapting the protocol used to produce the LAGG hydrogels, as schematized in Figure 10.

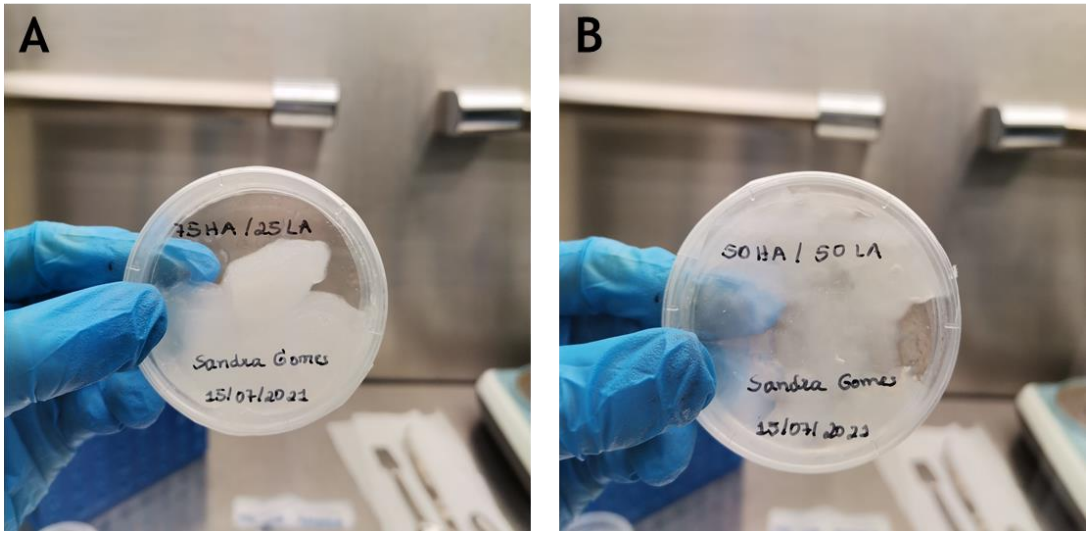


Figure 25. HAGG:LAGG hydrogels. (A) 75HAGG:25LAGG; (B) 50HAGG:50LAGG.

HAGG hydrogels and hydrogels with a mixture of high acyl gellan gum and low acyl gellan gum in different ratios (HAGG:LAGG hydrogels) were successfully produced. However, 75HAGG:25LAGG and 50HAGG:50LAGG hydrogels started to solidify while the mixture was still being poured into the Petri dishes and it was not possible to obtain a homogeneous, well dispersed hydrogel (Figure 25). Therefore, only HAGG (100HAGG), 25HAGG:75LAGG and 12.5HAGG:87.5LAGG hydrogels and hydrogels loaded with 10% w/v NLC (NLC-100HAGG, NLC-25HAGG:75LAGG and 12.5HAGG:87.5LAGG) were used in further tests.

3.5.2. HAGG:LAGG hydrogels' stability

To access their stability, 100HAGG, 25HAGG:75LAGG and 12.5HAGG:87.5LAGG hydrogels' discs (with and without NLC) were incubated at pH 7.4 and pH 2.6 for 24 h. Weight and diameter were measured before and after incubation. LAGG 2% hydrogels (100% LAGG) were used as control.

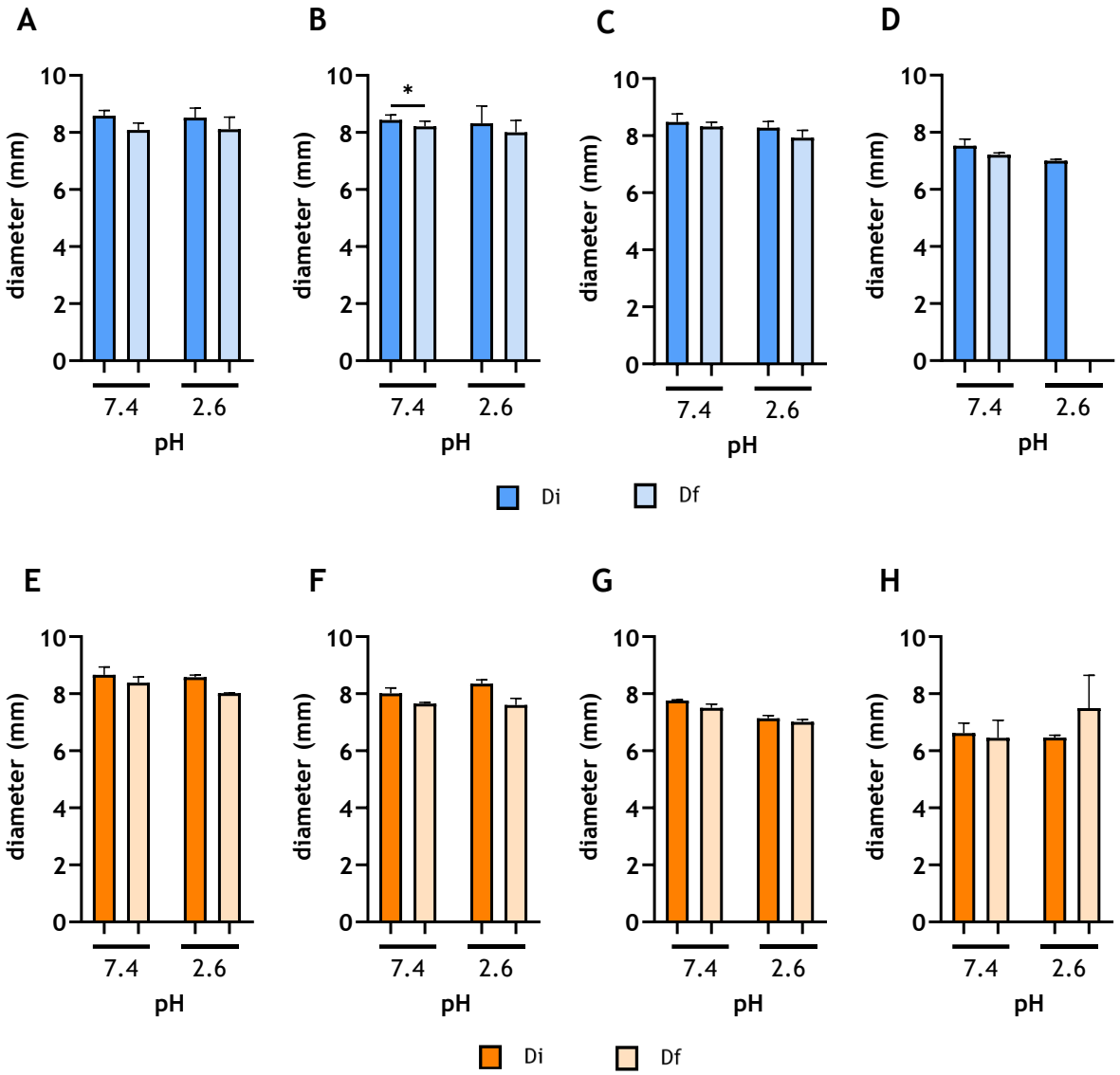


Figure 26. LAGG 2% (100LAGG), 100HAGG and HAGG:LAGG hydrogel's diameter. (A) LAGG 2% (100LAGG); (B) 12.5HAGG:87.5LAGG; (C) 25HAGG:75LAGG; (D) 100HAGG; (E) NLC-LAGG 2% (NLC-100LA); (F) NLC-12.5HAGG:87.5LAGG; (G) NLC-25HAGG:75LAGG; (H) NLC-100HAGG. Hydrogels' discs were incubated in pH 7.4 and pH 2.6, for 24 h, at 37°C, under agitation (150 rpm). Diameter was measured before (Di) and after (Df) incubation (t test; * - significantly different from each other, $p<0.05$; n=2).

After 24 h of incubation, the diameter of the hydrogels remained unaltered, with no significant variations (Figure 26). However, at pH 2.6 it was not possible to measure the diameter of 100HAGG hydrogels because they did not have mechanical properties to withstand the collection of the supernatant.

Regarding the weight, all hydrogels presented weight variation according to the pH of the medium (Figure 27).

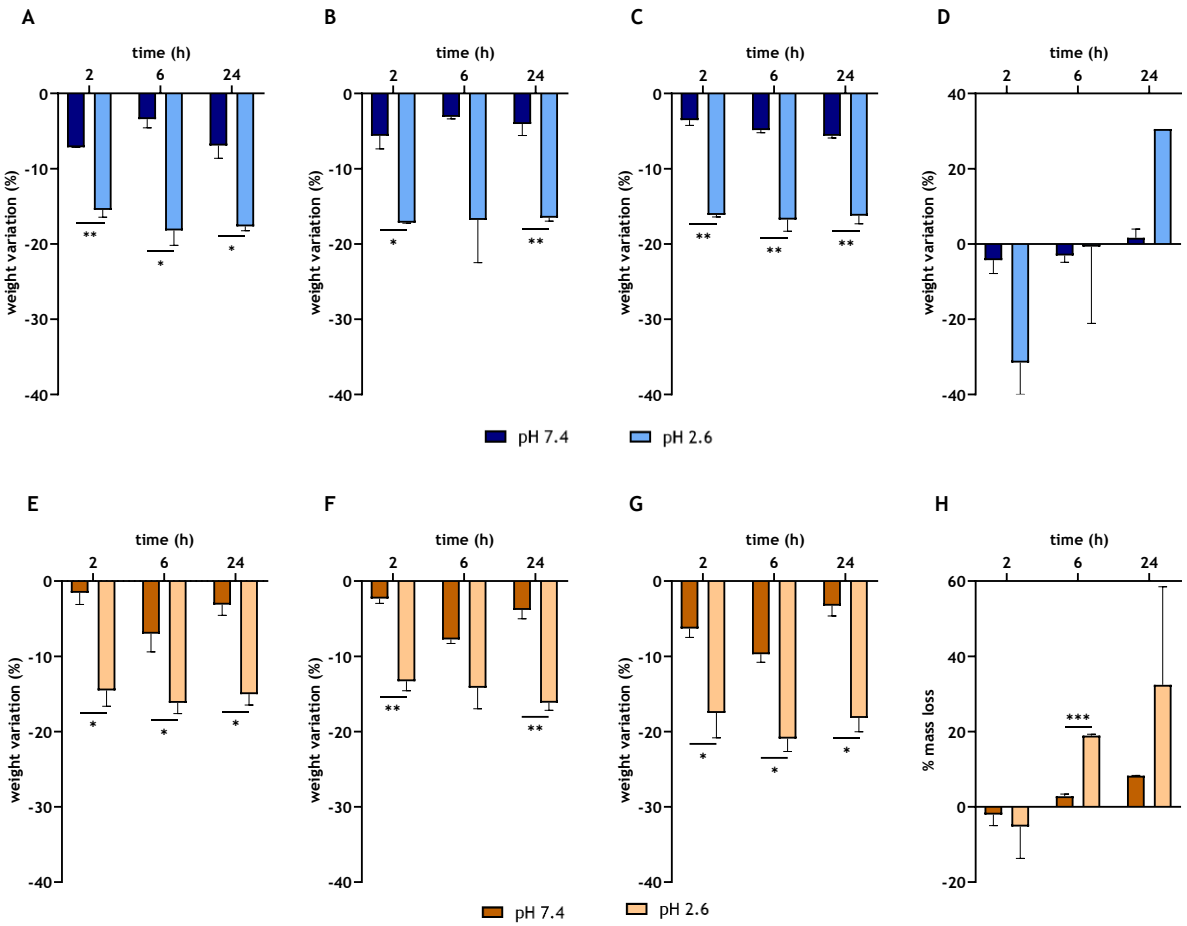


Figure 27. Stability of LAGG 2% (100LAGG), 100HAGG and HAGG:LAGG hydrogels in different pH conditions. (A) LAGG 2% (100LAGG); (B) 12.5HAGG:87.5LAGG; (C) 25HAGG:75LAGG; (D) 100HAGG; (E) NLC-LAGG 2% (NLC-100LAGG); (F) NLC-12.5HAGG:87.5LAGG; (G) NLC-25HAGG:75LAGG; (H) NLC-100HAGG. Hydrogel's discs were incubated in pH 7.4 and pH 2.6 for 24 h, at 37°C, under agitation (150 rpm). Weight was measured before and after incubation (t-test; *,**,*** - significantly different from each other, $p<0.05$, $p<0.01$, $p<0.001$, respectively; n=2).

LAGG 2% (100LAGG), 12.5HAGG:87.5LAGG and 25HAGG:75LAGG had a similar behavior, with similar mass loss in all conditions tested (Figure 27 A, B, C). Interestingly, 100HAGG (Figure 27D) presented a different pattern of weight variation from all the others: in the first hours of incubation occurred a reduction in the weight but after nearly 6 h of incubation this tendency changed, and it was observed an increase in their weight.

The addition of NLC had no effect on the overall hydrogel's stability, except for the 100HAGG hydrogels, where the addition of NLC seems to anticipate the weight increase (Figure 27H).

Despite 100HAGG hydrogels being the only ones that presented a different behavior from LAGG 2% (100LAGG) hydrogels, they were easily destroyed, i.e., they did not endure mechanical forces such as the ones induced by pipetting, at both pH 7.4 and pH 2.6 (Figure 28).

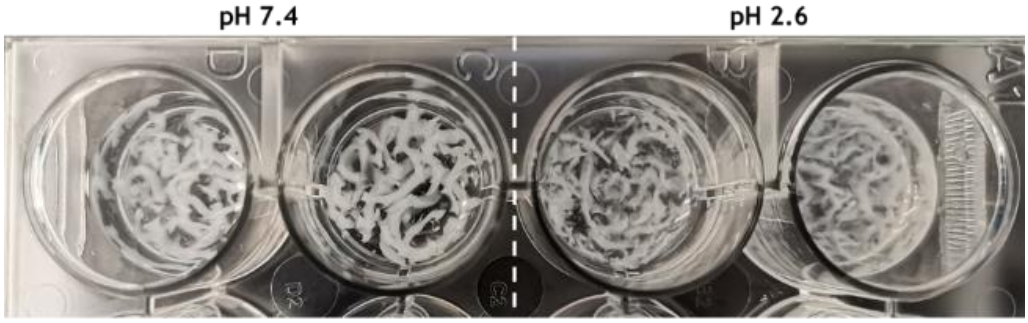


Figure 28. 100HAGG hydrogels after pipetting. Image of 100HAGG hydrogel's discs after 24 h of incubation at pH 7.4 and pH 2.6 when pipetting forces were applied to the supernatant.

3.5.3. HAGG:LAGG hydrogels' mechanical behavior

To access the mechanical behavior of the "mixed" hydrogels, as well as of the 100HAGG hydrogels (with and without nanoparticles), a DMA test using the same parameters previously applied to the LAGG hydrogels was performed. The obtained results are presented in Figure 29.

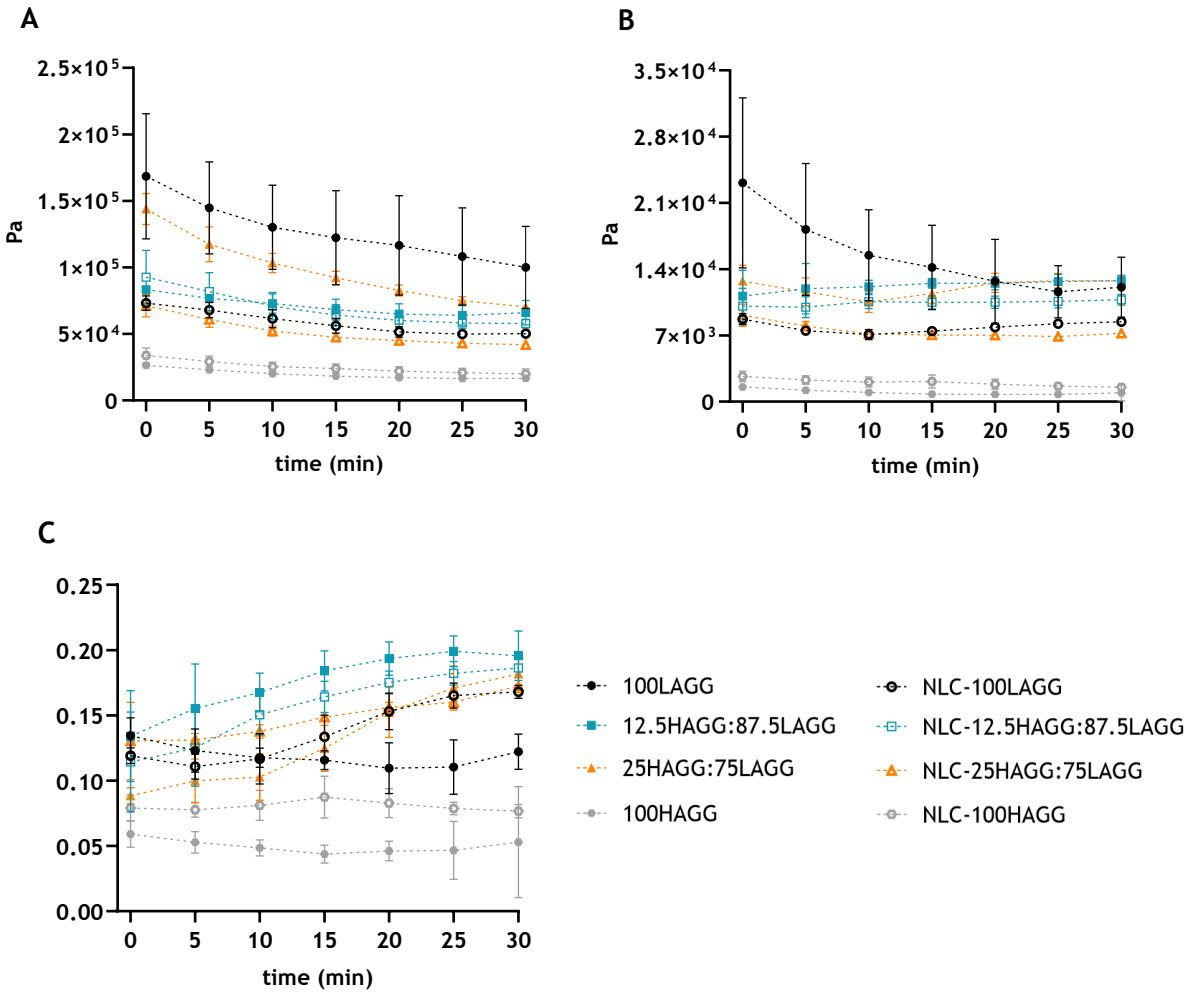


Figure 29. Mechanical behavior of LAGG 2% (100LAGG), 100HAGG and HAGG:LAGG hydrogels. (A) storage modulus, (B) loss modulus and (C) tan δ were accessed by DMA, compressing both the hydrogel's discs with a frequency of 0.05 Hz and a displacement of 0.04 ± 0.01 mm, for 30 min, at 37°C (n=3).

In general, both storage and loss moduli remained stable during the period of the experiment. The addition of NLC did not affect the mechanical properties of the hydrogels, except for the

25HAGG:75LAGG. For these, significant differences were observed in the storage modulus (Figure 28A) and on the loss modulus (Figure 28B) (from 20 to 30 minutes) between the hydrogels with and without NLC, with higher moduli obtained for the hydrogels without the nanoparticles. Again, all tested hydrogels presented a higher storage modulus than loss modulus (tan δ <1) (Figure 28C), which indicates an elastic behavior.

When comparing to the control hydrogels LAGG 2% (100LAGG), only NLC-100HAGG hydrogels presented a significant reduction in both storage and loss moduli. Furthermore, 100HAGG hydrogels showed a higher storage/loss ratio: while for the other hydrogels the ratio was never superior to 9, for NLC-100HAGG hydrogels the ratio was almost 13 and for 100HAGG hydrogels, the storage modulus was almost 23 times higher than the loss modulus.

3.5.4. NLC release from HAGG:LAGG hydrogels

The different hydrogels (LAGG 2% (100LAGG), 100HAGG and HAGG:LAGG hydrogels with and without NLC) were incubated in pH 7.4 and pH 2.6 over 24 h. Then, the supernatants were collected and analyzed by NTA. The theoretical quantity of NLC in each hydrogel's disc is presented in Table 9.

Table 9. Number of NLC in each disc of LAGG 2% (100LAGG), 100HAGG and HAGG:LAGG.

LAGG 2% (100LAGG)	12.5HAGG:87.5LAGG	25HAGG:75LAGG	100HAGG
$3.92x10^{11} \pm 1.36x10^{10}$	$3.61x10^{11} \pm 1.81x10^{10}$	$3.07x10^{11} \pm 2.61x10^{10}$	$2.46x10^{11} \pm 1.50x10^{10}$

The percentage of released nanoparticles are presented in Figure 30.

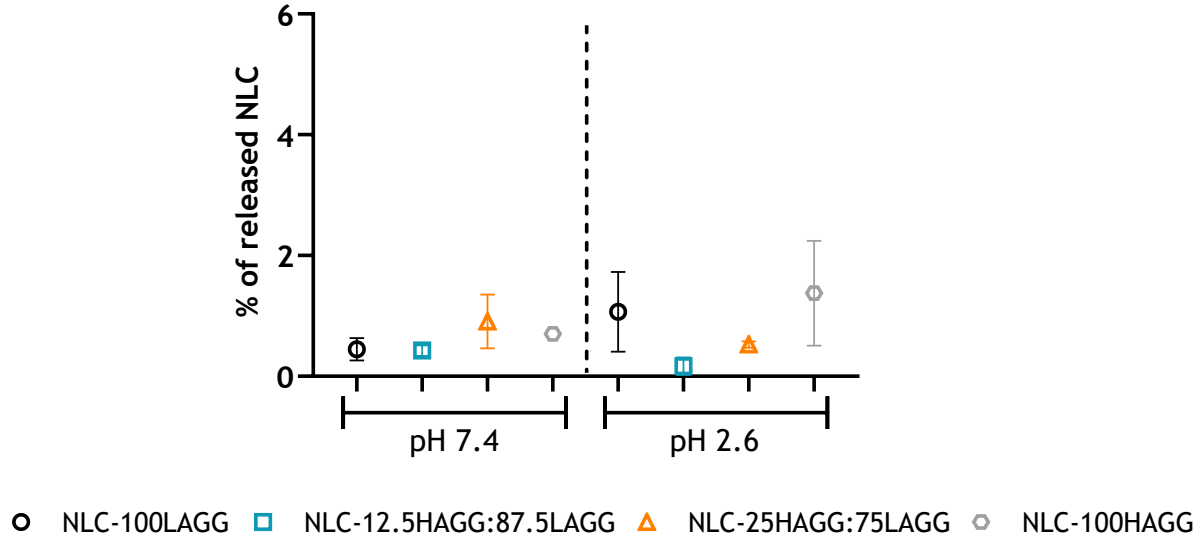


Figure 30. NLC release from LAGG 2% (100LAGG), 100HAGG and HAGG:LAGG hydrogels. Hydrogel's discs were incubated in pH 7.4 and pH 2.6, for 24 h, at 37°C, under agitation (150 rpm). Supernatants were collected to be analyzed by nanoparticle tracking analysis (n=2).

Table 10. Number of NLC released from LAGG 2% (100LAGG), 100HAGG and HAGG:LAGG hydrogels in different pH conditions. The number of nanoparticles that were release from hydrogel's discs was quantified by NTA after 24 h of incubation.

Hydrogels	pH 7.4	pH 2.6
LAGG 2% (100LAGG)	$1.75x10^9$	$4.16x10^9$
12.5HAGG:87.5LAGG	$1.47x10^9$	$6.15x10^8$
25HAGG:75LAGG	$3.02x10^9$	$1.48x10^9$
100HAGG	$1.78x10^9$	$3.33x10^9$

The preliminary results showed that, once again, the percentage of nanoparticles released at both pHs from the hydrogels tested was very low, which is translated in an insufficient number of NLC (Table 10) to achieve antimicrobial activity.

Chapter IV – Discussion

Helicobacter pylori has drawn attention since it was classified as a human carcinogenic agent by the IARC in 1994 [10]. Over the last 10 years, the resistance to the commonly used antibiotics to treat infection by this gastric pathogen has increased from 20 to 40%, leaving millions worldwide without effective therapy [29]. This high resistance rate has also been fueled by the lack of patient compliance to the complex therapeutic scheme used. Therefore, new non-antibiotic-based therapeutic strategies, with simpler regimens and more effective, are needed. Among the new options that have been object of research, docosahexaenoic acid (DHA), a polyunsaturated fatty acid, has emerged as a promising compound [55]. Seabra *et al*. designed nanostructured lipid carriers (NLC) and loaded them with DHA, aiming to improve the antimicrobial activity of the bioactive compound [56]. However, complete clearance of *H. pylori* infection *in vivo* using DHA-loaded NLC was achieved in only half of the animals and when administration was *ad libitum* (Seabra *et al*., manuscript in preparation).

Since the work herein described is a proof of concept for the development of a delivery system, only "bare" unloaded NLC (without DHA) were used. Nonetheless, these "bare" NLC also demonstrated antibacterial potential, although requiring more time to achieve the same outcome [56]. The diameter of the produced NLC was slightly higher when compared to the ones reported by Seabra *et al*. (302 nm vs the previously obtained 211 nm) [56]. It was previous reported by our group that the removal of the ultra-turrax step of the NLC production protocol did not significantly impact the NLC performance [133]. Therefore, this step was eliminated and this change from the original protocol might account for the diameter differences. It is noteworthy that this change intended to make the production process of NLC simpler, easier to scale-up and, in the long run, more cost-effective. Another factor that may also account to explain these differences is the fact that the production of the nanoparticles is a manual process, subjected to subtle differences according to the operator, which is reflected on the characteristics of the final produced NLC. Nevertheless, the surface charge of the nanoparticles was similar to the ones previously reported (-27 mV vs the reported -28 mV) and the low polydispersity index (~0.3) indicates that NLC present a homogenous size distribution [134]. Moreover, as expected and reported by Li *et al*. [135] and Mahajan *et al*. [136], the addition of coumarin-6 to the NLC structure for quantification protocols did not affect their properties, since no significant differences were observed in the parameters analyzed between NLC and cNLC. The encapsulation efficiency (EE) of coumarin-6 in NLC was estimated, in accordance with

our preliminary data, to be set at 96.4%. This parameter varies according to the composition of NLC and the drug/compound being encapsulated [137, 138]. It is possible to obtain very high EE using NLC [139, 140], especially for hydrophobic compounds due to the lipophilic components of these nanoparticles. Therefore, the obtained EE for coumarin-6, a hydrophobic compound, is in accordance with the literature.

The delivery system here designed for NLC delivery was based on gellan gum (GG). This polymer was chosen due to its water retention capacity, mucoadhesive properties and pH-responsive behavior [96], as well as its promising results as a drug delivery system for gastric settings [117-120, 122]. As a first approach, low acyl gellan gum (LAGG) hydrogels with different polymer concentrations were tested. Polymer concentration was chosen based on the work of Silva-Correia et al.[129], where LAGG hydrogels with a polymer concentration of 2% w/v were developed. Here, hydrogels with a polymer concentration of 1%, 1.5% and 2% w/v were successfully produced, both with and without nanoparticles in their composition. The lower polymer concentrations tested allowed to explore the influence of this parameter on the properties of the hydrogels, as well as on NLC's release. It was observed that the less concentrated hydrogels (LAGG 1.5%) presented poorer mechanical properties and released less nanoparticles than the more concentrated ones (LAGG 2%). Regarding LAGG 1% hydrogels, these could not endure the forces generated during hydrogel's cut. The more plausible explanation for this is that lower polymer concentrations are translated into lower crosslinking degrees, which generates mechanically weaker hydrogels [141]. As such, it was not possible to obtain LAGG 1% hydrogels' discs to use in further testing.

The stability tests in different pH conditions showed no significant differences in the hydrogels' diameter but concerning weight variation, a reduction was observed in all conditions tested. Although GG is described as stable and resistant to the acidic environment [96], it was observed a higher mass loss in lower pH conditions (specifically pH 2.6 and pH 1.2). Other studies have evaluated the weight variation of GG hydrogels, but all performed the analyzes using the dry weight of the hydrogels before and after incubation, i.e. the weight of lyophilized hydrogels, and not wet hydrogels as analyzed in this work [129, 142, 143]. LAGG and NLC-LAGG hydrogels had the same behavior, which led to the conclusion that both hydrogels have similar characteristics and that the addition of NLC did not interfere with weight and diameter changes.

The hydrogels' mechanical properties were studied with DMA technique. DMA allows to extract properties of polymers as function of different parameters, such as temperature, time and frequency. Briefly, a DMA analysis consists on the application of a sinusoidal oscillating stress, followed by measuring the material response that is a sinusoidal oscillation with similar frequency. If the material responds to the applied stress perfectly elastically, the material response is in-phase with the applied loading, while a perfectly viscous response corresponds to an out-of-phase wave [132]. Since polymers are viscoelastic materials, they respond to the applied stress in two ways: an elastic response (storage modulus), important for shape recovery, and a viscous response (loss modulus), related to the dispersion of mechanical energy, which is fundamental to prevent breakage. The phase angle (δ)

corresponds to the degree to which the stress response of the material is out of phase with the strain input [144]. The mechanical behavior analysis of the hydrogels highlighted the viscoelastic properties of the GG polymer, as they were capable to both store and dissipate energy, but a higher contribution from the elastic component was observed (higher storage modulus). Therefore, LAGG hydrogels (2 and 1.5%) presented an elastic behavior. Regarding the addition of NLC to the hydrogels, some authors have developed similar systems, i.e. nanoparticles encapsulated in hydrogels, and analyzed the effect of the addition of the nanoparticles in the mechanical properties of the hydrogels. Moorcroft *et al.* [145] developed a polyethylene glycol hydrogel to encapsulate peptide-loaded liposomes and gold nanorods and observed that the addition of the nanoparticles reduced both storage and loss moduli. Cleetus *et al.* [146] used alginate hydrogels to encapsulate ZnO nanoparticles at different concentrations and concluded that their mechanical properties varied according to the concentration of the nanoparticles, with higher % of ZnO leading to increased storage and loss moduli as a result of the crosslinking provided by zinc ions on alginate. Therefore, the addition of the nanoparticles to the hydrogels structure may alter their mechanical properties depending on the nanoparticles' concentration and interactions with the polymer. In this work, the addition of NLC did not impact the mechanical properties of the LAGG hydrogels as similar values were obtained between LAGG hydrogels and NLC-LAGG at the same polymer concentration. Regarding polymer concentration, more concentrated hydrogels (LAGG 2%) presented higher values for both moduli. This may be explained by the differences in the crosslinking degree: hydrogels with higher polymer concentration also have higher crosslinking density, which leads to an increase in both storage and loss moduli [141], which is in accordance with the obtained results. To date, no DMA analysis of LAGG hydrogels using a compression frequency of 0.05 Hz was found. This frequency was chosen to simulate the contractile forces of the stomach, about three contractions per minute [130]. However, some studies analyzed the mechanical behavior of LAGG hydrogels with a polymer concentration of 2% but within a frequency range of 0.1Hz as the lowest frequency. As this value is very close to the frequency used in this work, it is possible to estimate that the values at 0.05 Hz would be within the same range. Although a slight increase was observed in the storage modulus with increasing frequencies, the differences were practically residual, since the values remained between $1x10^5$Pa and $2x10^5$ Pa [129, 142]. Therefore, the values obtained in these studies with a frequency of 0.1 Hz are in accordance with the obtained storage modulus for LAGG 2% hydrogels studied in this work.

Another important aspect to obtain a proper delivery system is how well NLC are dispersed on the hydrogel mesh. To analyse that, confocal microscopy was used by taking advantage of the fluorescent properties of coumarin-6 loaded-NLC. Images revealed a uniform distribution of the nanoparticles in LAGG hydrogels in both polymer's concentration (2% and 1.5%). This is an important aspect to achieve a controlled sustained release of the nanoparticles: the nanoparticles closer to the surface of the hydrogel are first delivered, followed by a sustained release of the more internal ones. In theory, this allows to maintain therapeutic concentrations in the site of action for prolonged periods of time. As

such, it is expected that, based on the NLC dispersion, the designed system would allow a sustained NLC release on the stomach.

NLC released over incubation at different settings (pH and incubation time) was performed using two distinct techniques: fluorescence analysis (using coumarin-6-loaded NLC) and nanoparticle tracking analysis (NTA). Fluorimetry is based on the measure of a specific wavelength that is emitted from a particular compound (emission wavelength) previously excited with a specific wavelength (excitation wavelength). The fluorescence intensity detected can be converted into sample concentration and the main advantages of fluorimetry are its high sensitivity and specificity [147], while it is also a simple, economic and fast method [148]. However, this technique presents some drawbacks as it can only detect fluorescent compounds, it is highly dependent on environmental factors, such as pH and ionic strength, the radiation used to excite the sample can damage the fluorescent compound and the interactions between the fluorophore and other substances can reduce the fluorescence (quenching phenomena) [147]. Also, it is an indirect method, since NLC quantification is obtained by the conversion of fluorescence intensity into NLC concentration rather than by the direct count of the nanoparticles. The other technique used, NTA, consists in a multiparameter analysis of nanoparticles in liquid suspensions that allows their quantification, visualization and diameter measurement [149]. The liquid sample is injected into a sample cell and illuminated by a laser, allowing the nanoparticles visualization and quantification due to light scattering and the movement of the nanoparticles allows to measure their diameter [150].The main advantage of this method is to allow a direct quantification of the nanoparticles, with real-time visualization of the sample. However, samples must be within a certain concentration and the parameter settings defined can influence the results obtained [150]. Both techniques showed that LAGG hydrogels (2% and 1.5%) could release the nanoparticles, although in a very low percentage (less than 6%). This low release could be associated with electrostatic interactions between the nanoparticles and the GG polymer. However, GG is negatively charged above pH 3.0 [151]. Since NLC are also negatively charged, electrostatic interactions cannot account for the low NLC release. A slight discrepancy was observed on the number of NLC released between the two quantification methods. This difference was more pronounced in pH 2.6 ($5.11x10^9$ NLC (fluorescence) vs $5.32x10^8$ NLC (NTA) for NLC-LAGG 2% hydrogels and $2.10x10^9$ NLC (fluorescence) vs $1.76x10^8$ NLC (NTA) for NLC-LAGG 1.5% hydrogels), which can be explained by the differences in the two techniques, as mentioned above, but mostly because pH affects the fluorescence readings. The release of NLC was higher for the LAGG 2% hydrogels (more concentrated). When the polymer concentration is higher, the crosslinking degree is also higher and, in theory, that should be translated in a more compact structure that hampers the release of the nanoparticles. However, this was not observed, since a higher release was observed in the NLC-LAGG 2% / cNLC-LAGG 2% hydrogels comparing to NLC-LAGG 1.5% / cNLC-LAGG 1.5% hydrogels. Also, a higher crosslinking degree leads to a decrease in the swelling capacity of hydrogels [152] and, although the swelling behavior of hydrogels was not evaluated, it is expected that LAGG 1.5% hydrogels have higher swelling ratio comparing to LAGG 2% hydrogels. In the

literature, it is commonly claimed that higher swelling ratios and lower polymer concentration facilitate drug release from the hydrogel [153-157]. However, some authors also state that the swelling of the hydrogel structure can hamper the compounds diffusion to the medium, which might explain the higher NLC release observed for the NLC-LAGG 2% hydrogels than on the 1.5% ones [96, 158]. Nonetheless, and even after 72 h of incubation in harsh pH settings (pH 1.2 and pH 2.6), the number of NLC released from both LAGG 2% and LAGG 1.5% was not enough to reach bactericidal effect, which is observed at 10^{12} particles/mL [133]. After 72 h, the maximum amount of NLC released was 2.90×10^{9} at pH 7.4 and for the LAGG 2% hydrogels. The antimicrobial preliminary tests confirmed that the hydrogels *per se* had no antibacterial activity, which is in accordance with what was reported in the literature [159, 160]. The antibacterial screening of hydrogel's extracts also confirmed that the amount of NLC released was not enough to have any effect on *H. pylori* cells.

Therefore, hydrogel optimization was required to improve the release of NLC and achieve bactericidal levels. For that, a second approach was developed: high acyl gellan gum (HAGG) was mixed with LAGG. HAGG generates less compact structures, with higher swelling behavior, and ideally it would facilitate the nanoparticles' release. Mixed hydrogels (HAGG and LAGG) with different ratios (25HAGG:75LAGG & 12.5HAGG:87.5LAGG), as well as 100% HAGG hydrogels, were successfully produced, both with and without NLC. Regarding the stability of the mixed HAGG:LAGG hydrogels, similar behavior was observed when compared to pure LAGG 2% hydrogels, i.e., mass loss was observed for all conditions tested, being higher for more acidic mediums. However, for HAGG hydrogels (both with and without NLC) it was observed a weight reduction in the first hours (6 h), followed by an increase in the mass of the hydrogels up to 24 h, which may be linked to swelling of the hydrogel. Although the swelling behavior was not accessed in this work, GG, specially HAGG, is described in the literature as having a high swelling ability [102]. Concerning the mechanical behavior, only NLC-100HAGG hydrogels had different storage and loss moduli from the LAGG 2% hydrogels, with an increase in the storage/loss ratio for 100HAGG and NLC-100HAGG hydrogels. This ratio translates the relative contributions of both elastic and viscous mechanisms in the material's response: the higher the storage/loss ratio, the higher the contribution of the elastic component [132]. As described earlier, LAGG produces hard and brittle gels due to a highly effective packing. However, due to the presence of a higher number of available acyl groups, the hydrogels prepared with HAGG present a less effective packing, resulting in more soft and elastic hydrogels [96]. Therefore, the relative contribution of the elastic component in the overall response of HAGG hydrogels will be higher than in LAGG hydrogels. This higher contribution could be advantageous for the desired application, taking in consideration the peristaltic movements that occur in the stomach, as it would allow the hydrogel to retain its shape. However, HAGG hydrogels proved to be mechanically weaker than all other formulations tested (as demonstrated by the lower storage modulus together with easy destruction by mechanical forces such as the ones induce by pipetting), which can facilitate their destruction in the gastric environment. Finally, preliminary release results demonstrated that both 100HAGG and mixed HAGG:LAGG hydrogels in all ratios have a low NLC release (less than 2%), similar to what was

obtained with the LAGG hydrogels. Therefore, although the designed hydrogels (LAGG 2% and HAGG/HAGG:LAGG) are fit for the intended application of NLC sustained released on the stomach, the NLC release profile must be fine-tuned to achieve bactericidal effect and become an useful "weapon" to counteract *H. pylori* infection.

Chapter V – Conclusion

In this work, gellan gum hydrogels were designed as a gastric delivery system for nanostructured lipid carriers (NLC), aiming to increase their residence time on the stomach. It is the first time that a combination of NLC and gellan gum in the context of *H. pylori* infection is reported.

Low acyl gellan gum (LAGG) hydrogels presented a pH-dependent stability and showed good mechanical properties. Also, they were able to release the nanoparticles, although not in the required NLC concentration to achieve a bactericidal effect against *H. pylori* J99. The addition of high acyl gellan gum (HAGG) to the hydrogel's structure was not sufficient to improve the NLC's release.

The obtained results showed that the designed formulations are a good strategy to pursue to encapsulate NLC, since the hydrogels' properties, namely the stability and the elastic behavior, are not affected by their addition. However, this strategy needs further optimization to fine-tune the NLC release to achieve bactericidal levels and become a promising strategy for *H. pylori* eradication.

Chapter VI – Future Perspectives

There are several aspects that could be improved to enhance the performance of the designed hydrogels for gastric delivery of NLC.

First and before changing the hydrogel's formulation parameters, it would be interesting to incubate the hydrogels' discs in higher volumes. This would allow to confirm that the low release of the NLC is due to the hydrogel's constrains and not because the solubility limit of the nanoparticles has been reached. Then, it could also be explored an increase on the initial amount of NLC that are incorporated, without compromising the hydrogels' stability or mechanical behavior, since a higher cargo tends to lead to an increase in the quantity of the compound that is released [161]. Another possible strategy is the chemical modification of gellan gum. For instance, sericin has shown to be efficient in increasing drug release in more acidic pH when mixed with gellan gum by increasing the hydrogels' swelling due to its pH-sensitive aminoacids [103, 104]. Therefore, the modification of the polymer structure with pH-responsive molecules may be a promising approach to boost the nanoparticles release through diffusion in the environment of the stomach. The degradation rate of GG can also be tuned to increase the release of NLC, but always bearing in mind that the formulation is intended to remain in the stomach for defined periods of time, ideally a few days.

After adjusting the delivery system to an optimal formulation, its antibacterial properties need to be tested, as well as the cytotoxicity of the components of the delivery system, according to ISO standards (ISO 10993, especially parts 5 and 12). Also, and considering a possible translational research path, an important aspect to be analyzed is the shelf-life of the hydrogels and their storage requirements.

Finally, the ultimate goal would be, after full *in vitro* optimization is performed and the feasibility/safety of the selected delivery system is established, to demonstrate *in vivo* that resourcing to gellan gum hydrogels to deliver NLC boosts their overall performance and that full clearance of *H. pylori* infection is possible to be achieved.

References

1. Zamani, M., et al., *Systematic review with meta-analysis: the worldwide prevalence of Helicobacter pylori infection.* Aliment Pharmacol Ther, 2018. **47**(7): p. 868-876.
2. Mezmale, L., et al., *Review: Epidemiology of Helicobacter pylori.* Helicobacter, 2020. **25 Suppl 1**: p. e12734.
3. Hooi, J.K.Y., et al., *Global Prevalence of Helicobacter pylori Infection: Systematic Review and Meta-Analysis.* Gastroenterology, 2017. **153**(2): p. 420-429.
4. Sjomina, O., et al., *Epidemiology of Helicobacter pylori infection.* Helicobacter, 2018. **23 Suppl 1**: p. e12514.
5. Perry, S., et al., *Gastroenteritis and transmission of Helicobacter pylori infection in households.* Emerging infectious diseases, 2006. **12**(11): p. 1701-1708.
6. Azevedo, N.F., et al., *A new model for the transmission of Helicobacter pylori: role of environmental reservoirs as gene pools to increase strain diversity.* Crit Rev Microbiol, 2007. **33**(3): p. 157-69.
7. Brown, L.M., *Helicobacter pylori: epidemiology and routes of transmission.* Epidemiol Rev, 2000. **22**(2): p. 283-97.
8. Lopes, D., et al., *Eradication of Helicobacter pylori: Past, present and future.* J Control Release, 2014. **189**: p. 169-86.
9. Plummer, M., et al., *Global burden of gastric cancer attributable to Helicobacter pylori.* Int J Cancer, 2015. **136**(2): p. 487-90.
10. IARC, *Schistosomes, liver flukes and Helicobacter pylori.* IARC Monographs on the Evaluation of Carcinogenic Risks to Humans, 1994. **61**: p. 177-220.
11. Global Cancer Obervatory. *Cancer Today*. 2020 10 May 2021]; Available from: https://gco.iarc.fr/today/.
12. American Cancer Society. *Stomach Cancer Stages*. 2021 [cited 2021 July 19th]; Available from: https://www.cancer.org/cancer/stomach-cancer/detection-diagnosis-staging/staging.html.
13. Layke, J.C. and P.P. Lopez, *Gastric cancer: diagnosis and treatment options.* Am Fam Physician, 2004. **69**(5): p. 1133-40.
14. American Cancer Society. *Stomach Cancer Survival Rates*. 2021 [cited 2021 July 19th]; Available from: https://www.cancer.org/cancer/stomach-cancer/detection-diagnosis-staging/survival-rates.html.
15. Gu, H., *Role of Flagella in the Pathogenesis of Helicobacter pylori.* Current microbiology, 2017. **74**(7): p. 863-869.
16. Gupta, N., et al., *Unraveling the factors and mechanism involved in persistence: Host-pathogen interactions in Helicobacter pylori.* J Cell Biochem, 2019. **120**(11): p. 18572-18587.
17. Radosz-Komoniewska, H., et al., *Pathogenicity of Helicobacter pylori infection.* Clin Microbiol Infect, 2005. **11**(8): p. 602-10.
18. Kobayashi, M., et al., *Carbohydrate-dependent defense mechanisms against Helicobacter pylori infection.* Current drug metabolism, 2009. **10**(1): p. 29-40.
19. Aspholm-Hurtig, M., et al., *Functional adaptation of BabA, the H. pylori ABO blood group antigen binding adhesin.* Science, 2004. **305**(5683): p. 519-22.
20. Ilver, D., et al., *Helicobacter pylori adhesin binding fucosylated histo-blood group antigens revealed by retagging.* Science, 1998. **279**(5349): p. 373-7.

21. Kable, M.E., et al., *Host Determinants of Expression of the Helicobacter pylori BabA Adhesin.* Scientific Reports, 2017. **7**(1): p. 46499.
22. Goodwin, A.C., et al., *Expression of the Helicobacter pylori adhesin SabA is controlled via phase variation and the ArsRS signal transduction system.* Microbiology (Reading), 2008. **154**(Pt 8): p. 2231-2240.
23. Pérez-Pérez, G.I., et al., *Activation of human THP-1 cells and rat bone marrow-derived macrophages by Helicobacter pylori lipopolysaccharide.* Infection and immunity, 1995. **63**(4): p. 1183-1187.
24. Algood, H.M.S. and T.L. Cover, *Helicobacter pylori persistence: an overview of interactions between H. pylori and host immune defenses.* Clinical microbiology reviews, 2006. **19**(4): p. 597-613.
25. de Bernard, M., et al., *Helicobacter pylori toxin VacA induces vacuole formation by acting in the cell cytosol.* Mol Microbiol, 1997. **26**(4): p. 665-74.
26. Monstein, H.J. and J. Jonasson, *Differential virulence-gene mRNA expression in coccoid forms of Helicobacter pylori.* Biochem Biophys Res Commun, 2001. **285**(2): p. 530-6.
27. Wang, X.F. and K.X. Wang, *Cloning and expression of vacA gene fragment of Helicobacter pylori with coccoid form.* J Chin Med Assoc, 2004. **67**(11): p. 549-56.
28. Wen, M., et al., *An evaluative system for the response of antibacterial therapy: based on the morphological change of Helicobacter pylori and mucosal inflammation.* Pathol Int, 1999. **49**(4): p. 332-7.
29. Dang, B.N. and D.Y. Graham, *Helicobacter pylori infection and antibiotic resistance: a WHO high priority?* Nat Rev Gastroenterol Hepatol, 2017. **14**(7): p. 383-384.
30. WHO. *GLOBAL PRIORITY LIST OF ANTIBIOTIC-RESISTANT BACTERIA TO GUIDE RESEARCH, DISCOVERY, AND DEVELOPMENT OF NEW ANTIBIOTICS*. 2017 [cited 2021 July 1st]; Available from: https://www.who.int/medicines/publications/WHO-PPL-Short_Summary_25Feb-ET_NM_WHO.pdf?ua=1.
31. Malfertheiner, P., et al., *Management of Helicobacter pylori infection—the Maastricht V/Florence Consensus Report.* Gut, 2017. **66**(1): p. 6-30.
32. Chey, W.D., et al., *ACG Clinical Guideline: Treatment of Helicobacter pylori Infection.* Official journal of the American College of Gastroenterology | ACG, 2017. **112**(2): p. 212-239.
33. Fallone, C.A., et al., *The Toronto Consensus for the Treatment of Helicobacter pylori Infection in Adults.* Gastroenterology, 2016. **151**(1): p. 51-69.e14.
34. Vakil, N., *Helicobacter pylori treatment: a practical approach.* Am J Gastroenterol, 2006. **101**(3): p. 497-9.
35. Koivisto, T.T., et al., *First-line eradication therapy for Helicobacter pylori in primary health care based on antibiotic resistance: results of three eradication regimens.* Aliment Pharmacol Ther, 2005. **21**(6): p. 773-82.
36. Suzuki, T., et al., *Smoking increases the treatment failure for Helicobacter pylori eradication.* Am J Med, 2006. **119**(3): p. 217-24.
37. Lei, J., et al., *The antimicrobial peptides and their potential clinical applications.* American journal of translational research, 2019. **11**(7): p. 3919-3931.
38. Chen, L., et al., *An antimicrobial peptide with antimicrobial activity against Helicobacter pylori.* Peptides, 2007. **28**(8): p. 1527-31.
39. Ge, Y., et al., *In vitro antibacterial properties of pexiganan, an analog of magainin.* Antimicrob Agents Chemother, 1999. **43**(4): p. 782-8.
40. Parreira, P., et al., *Helicobacter pylori infection: A brief overview on alternative natural treatments to conventional therapy.* Crit Rev Microbiol, 2016. **42**(1): p. 94-105.
41. Parreira, P., et al., *Surface Grafted MSI-78A Antimicrobial Peptide has High Potential for Gastric Infection Management.* Scientific Reports, 2019. **9**(1): p. 18212.
42. Baker, D.A., *Plants against Helicobacter pylori to combat resistance: An ethnopharmacological review.* Biotechnology Reports, 2020. **26**: p. e00470.
43. Parreira, P., et al., *Eucalyptus spp. outer bark extracts inhibit Helicobacter pylori growth: in vitro studies.* Industrial Crops and Products, 2017. **105**: p. 207-214.
44. Romero, C., et al., *In vitro activity of olive oil polyphenols against Helicobacter pylori.* J Agric Food Chem, 2007. **55**(3): p. 680-6.
45. Mahady, G.B., S.L. Pendland, and L.R. Chadwick, *Resveratrol and red wine extracts inhibit the growth of CagA+ strains of Helicobacter pylori in vitro.* Am J Gastroenterol, 2003. **98**(6): p. 1440-1.

46. Paulo, L., et al., *Anti-Helicobacter pylori and urease inhibitory activities of resveratrol and red wine*. Food Research International, 2011. **44**: p. 964-969.
47. Parreira, P., et al., *Bioengineered surfaces promote specific protein–glycan mediated binding of the gastric pathogen Helicobacter pylori*. Acta Biomaterialia, 2013. **9**(11): p. 8885-8893.
48. Gonçalves, I.C., et al., *Bacterial-binding chitosan microspheres for gastric infection treatment and prevention*. Acta Biomater, 2013. **9**(12): p. 9370-8.
49. Henriques, P.C., et al., *Orally administrated chitosan microspheres bind Helicobacter pylori and decrease gastric infection in mice*. Acta Biomater, 2020. **114**: p. 206-220.
50. Gopal, G.J., et al., *Molecular characterization and polyclonal antibody generation against core component CagX protein of Helicobacter pylori type IV secretion system*. Bioengineered, 2014. **5**(2): p. 107-113.
51. Ardekani, L.S., et al., *A novel nanobody against urease activity of Helicobacter pylori*. International Journal of Infectious Diseases, 2013. **17**(9): p. e723-e728.
52. Sun, C.Q., C.J. O'Connor, and A.M. Roberton, *Antibacterial actions of fatty acids and monoglycerides against Helicobacter pylori*. FEMS Immunol Med Microbiol, 2003. **36**(1-2): p. 9-17.
53. Bergsson, G., O. Steingrímsson, and H. Thormar, *Bactericidal effects of fatty acids and monoglycerides on Helicobacter pylori*. Int J Antimicrob Agents, 2002. **20**(4): p. 258-62.
54. Thompson, L., A. Cockayne, and R.C. Spiller, *Inhibitory effect of polyunsaturated fatty acids on the growth of Helicobacter pylori: a possible explanation of the effect of diet on peptic ulceration*. Gut, 1994. **35**(11): p. 1557-1561.
55. Correia, M., et al., *Docosahexaenoic acid inhibits Helicobacter pylori growth in vitro and mice gastric mucosa colonization*. PLoS One, 2012. **7**(4): p. e35072.
56. Seabra, C.L., et al., *Docosahexaenoic acid loaded lipid nanoparticles with bactericidal activity against Helicobacter pylori*. Int J Pharm, 2017. **519**(1-2): p. 128-137.
57. Müller, R.H. and J.S. Lucks, *Medication vehicles made of solid lipid particles (solid lipid nanospheres - sln)*. European Patent EP0605497B1, 1996.
58. Gasco, M.R., *Method for producing solid lipid microspheres having a narrow size distribution*. US Patent No 5250236A, 1993.
59. Wissing, S.A., O. Kayser, and R.H. Muller, *Solid lipid nanoparticles for parenteral drug delivery*. Adv Drug Deliv Rev, 2004. **56**(9): p. 1257-72.
60. Pimentel-Moral, S., et al., *Lipid nanocarriers for the loading of polyphenols – A comprehensive review*. Advances in Colloid and Interface Science, 2018. **260**: p. 85-94.
61. Müller, R.H., K. Mäder, and S. Gohla, *Solid lipid nanoparticles (SLN) for controlled drug delivery – a review of the state of the art*. European Journal of Pharmaceutics and Biopharmaceutics, 2000. **50**(1): p. 161-177.
62. Mishra, V., et al., *Solid Lipid Nanoparticles: Emerging Colloidal Nano Drug Delivery Systems*. Pharmaceutics, 2018. **10**(4): p. 191.
63. Dhiman, N., et al., *Lipid Nanoparticles as Carriers for Bioactive Delivery*. Frontiers in chemistry, 2021. **9**: p. 580118-580118.
64. Mehnert, W. and K. Mäder, *Solid lipid nanoparticles: Production, characterization and applications*. Advanced Drug Delivery Reviews, 2001. **47**(2): p. 165-196.
65. Westesen, K., H. Bunjes, and M.H.J. Koch, *Physicochemical characterization of lipid nanoparticles and evaluation of their drug loading capacity and sustained release potential*. Journal of Controlled Release, 1997. **48**(2-3): p. 223-236.
66. Müller, R.H., M. Radtke, and S.A. Wissing, *Nanostructured lipid matrices for improved microencapsulation of drugs*. International Journal of Pharmaceutics, 2002. **242**(1): p. 121-128.
67. Haider, M., et al., *Nanostructured Lipid Carriers for Delivery of Chemotherapeutics: A Review*. Pharmaceutics, 2020. **12**(3).
68. Kaur, S., et al., *Nanostructure Lipid Carrier (NLC): the new generation of lipid nanoparticles*. Asian Pacific Journal of Health Sciences, 2015. **2**: p. 76-93.
69. Jenning, V., A.F. Thünemann, and S.H. Gohla, *Characterisation of a novel solid lipid nanoparticle carrier system based on binary mixtures of liquid and solid lipids*. International Journal of Pharmaceutics, 2000. **199**(2): p. 167-177.
70. Neupane, Y.R., et al., *Lipid drug conjugate nanoparticle as a novel lipid nanocarrier for the oral delivery of decitabine: ex vivo gut permeation studies*. Nanotechnology, 2013. **24**(41): p. 415102.

71. Muchow, M., P. Maincent, and R.H. Muller, *Lipid nanoparticles with a solid matrix (SLN, NLC, LDC) for oral drug delivery.* Drug Dev Ind Pharm, 2008. **34**(12): p. 1394-405.
72. Gokce, E.H., et al., *Resveratrol-loaded solid lipid nanoparticles versus nanostructured lipid carriers: evaluation of antioxidant potential for dermal applications.* International journal of nanomedicine, 2012. **7**: p. 1841-1850.
73. Pinto, M.F., et al., *A new topical formulation for psoriasis: Development of methotrexate-loaded nanostructured lipid carriers.* International Journal of Pharmaceutics, 2014. **477**(1): p. 519-526.
74. Li, X., et al., *A controlled-release ocular delivery system for ibuprofen based on nanostructured lipid carriers.* International Journal of Pharmaceutics, 2008. **363**(1): p. 177-182.
75. Patlolla, R.R., et al., *Formulation, characterization and pulmonary deposition of nebulized celecoxib encapsulated nanostructured lipid carriers.* J Control Release, 2010. **144**(2): p. 233-41.
76. Shi, F., et al., *Formulation design, preparation, and in vitro and in vivo characterizations of β-Elemene-loaded nanostructured lipid carriers.* Int J Nanomedicine, 2013. **8**: p. 2533-41.
77. Seabra, C.L., et al., *Lipid nanoparticles to counteract gastric infection without affecting gut microbiota.* Eur J Pharm Biopharm, 2018. **127**: p. 378-386.
78. Tran, T.H., et al., *Preparation and characterization of fenofibrate-loaded nanostructured lipid carriers for oral bioavailability enhancement.* AAPS PharmSciTech, 2014. **15**(6): p. 1509-15.
79. Patil-Gadhe, A. and V. Pokharkar, *Montelukast-loaded nanostructured lipid carriers: Part I Oral bioavailability improvement.* European Journal of Pharmaceutics and Biopharmaceutics, 2014. **88**(1): p. 160-168.
80. Zhuang, C.-Y., et al., *Preparation and characterization of vinpocetine loaded nanostructured lipid carriers (NLC) for improved oral bioavailability.* International Journal of Pharmaceutics, 2010. **394**(1): p. 179-185.
81. Mandpe, L. and V. Pokharkar, *Quality by design approach to understand the process of optimization of iloperidone nanostructured lipid carriers for oral bioavailability enhancement.* Pharmaceutical Development and Technology, 2015. **20**(3): p. 320-329.
82. Elmowafy, M., et al., *Atorvastatin-loaded nanostructured lipid carriers (NLCs): strategy to overcome oral delivery drawbacks.* Drug Delivery, 2017. **24**(1): p. 932-941.
83. Murthy, A., et al., *Oral Bioavailability Enhancement of Raloxifene with Nanostructured Lipid Carriers.* Nanomaterials, 2020. **10**(6): p. 1085.
84. Huguet-Casquero, A., et al., *Oral delivery of oleuropein-loaded lipid nanocarriers alleviates inflammation and oxidative stress in acute colitis.* International Journal of Pharmaceutics, 2020. **586**: p. 119515.
85. Adebisi, A. and B.R. Conway, *Gastroretentive microparticles for drug delivery applications.* J Microencapsul, 2011. **28**(8): p. 689-708.
86. Lopes, C.M., et al., *Overview on gastroretentive drug delivery systems for improving drug bioavailability.* Int J Pharm, 2016. **510**(1): p. 144-58.
87. Salessiotis, N., *Measurement of the diameter of the pylorus in man. I. Experimental project for clinical application.* American journal of surgery, 1972. **124**(3): p. 331-333.
88. Klausner, E.A., et al., *Expandable gastroretentive dosage forms.* J Control Release, 2003. **90**(2): p. 143-62.
89. Liu, Z., et al., *In vitro and in vivo studies on mucoadhesive microspheres of amoxicillin.* J Control Release, 2005. **102**(1): p. 135-44.
90. Silva, M.M., et al., *Chitosan Nanoparticles as a Mucoadhesive Drug Delivery System for Ocular Administration.* Mar Drugs, 2017. **15**(12).
91. de Oliveira Cardoso, V.M., M.P.D. Gremiao, and B.S.F. Cury, *Mucin-polysaccharide interactions: A rheological approach to evaluate the effect of pH on the mucoadhesive properties.* Int J Biol Macromol, 2020. **149**: p. 234-245.
92. Rossi, A., et al., *Floating modular drug delivery systems with buoyancy independent of release mechanisms to sustain amoxicillin and clarithromycin intra-gastric concentrations.* Drug Dev Ind Pharm, 2016. **42**(2): p. 332-9.
93. Clarke, G.M., J.M. Newton, and M.B. Short, *Comparative gastrointestinal transit of pellet systems of varying density.* International Journal of Pharmaceutics, 1995. **114**(1): p. 1-11.

94. Murphy, C.S., et al., *Gastroretentive drug delivery systems: current developments in novel system design and evaluation.* Curr Drug Deliv, 2009. **6**(5): p. 451-60.
95. FDA. *Food Additives Permitted for Direct Addition to Food for Human Consuption. 21CFR172.665.* 2020 [cited 2021 June 28th]; Available from: https://www.accessdata.fda.gov/scripts/cdrh/cfdocs/cfcfr/cfrsearch.cfm?fr=172.665.
96. Milivojevic, M., et al., *Gellan gum in drug delivery applications*, in *Natural Polysaccharides in Drug Delivery and Biomedical Applications*. 2019. p. 145-186.
97. Nag, A., K.-S. Han, and H. Singh, *Microencapsulation of probiotic bacteria using pH-induced gelation of sodium caseinate and gellan gum.* International Dairy Journal, 2011. **21**(4): p. 247-253.
98. Matricardi, P., et al., *Preparation and characterization of novel gellan gum hydrogels suitable for modified drug release.* Molecules, 2009. **14**(9): p. 3376-91.
99. Palumbo, F.S., et al., *Gellan gum-based delivery systems of therapeutic agents and cells.* Carbohydr Polym, 2019. **229**: p. 115430.
100. Kirchmajer, D.M., et al., *Enhanced gelation properties of purified gellan gum.* Carbohydr Res, 2014. **388**: p. 125-9.
101. Horinaka, J., et al., *Effect of pH on the conformation of gellan chains in aqueous systems.* Biophys Chem, 2004. **111**(3): p. 223-7.
102. De Silva, D.A., et al., *Mechanical characteristics of swollen gellan gum hydrogels.* Journal of Applied Polymer Science, 2013. **130**(5): p. 3374-3383.
103. Arjama, M., et al., *Sericin/RBA embedded gellan gum based smart nanosystem for pH responsive drug delivery.* Int J Biol Macromol, 2018. **120**(Pt B): p. 1561-1571.
104. Mehnath, S., et al., *Sericin-chitosan doped maleate gellan gum nanocomposites for effective cell damage in Mycobacterium tuberculosis.* International Journal of Biological Macromolecules, 2019. **122**: p. 174-184.
105. Silva, N.A., et al., *The effects of peptide modified gellan gum and olfactory ensheathing glia cells on neural stem/progenitor cell fate.* Biomaterials, 2012. **33**(27): p. 6345-6354.
106. Ahearne, M. and D.J. Kelly, *A comparison of fibrin, agarose and gellan gum hydrogels as carriers of stem cells and growth factor delivery microspheres for cartilage regeneration.* Biomed Mater, 2013. **8**(3): p. 035004.
107. López-Cebral, R., et al., *Gellan gum based physical hydrogels incorporating highly valuable endogen molecules and associating BMP-2 as bone formation platforms.* Carbohydrate Polymers, 2017. **167**: p. 345-355.
108. Bhattacharya, S.S., et al., *Tranexamic acid loaded gellan gum-based polymeric microbeads for controlled release: In vitro and in vivo assessment.* Colloids and Surfaces B: Biointerfaces, 2013. **112**: p. 483-491.
109. Sun, J. and Z. Zhou, *A novel ocular delivery of brinzolamide based on gellan gum: in vitro and in vivo evaluation.* Drug Des Devel Ther, 2018. **12**: p. 383-389.
110. Kiani, H., et al., *Effect of gellan, alone and in combination with high-methoxy pectin, on the structure and stability of doogh, a yogurt-based Iranian drink.* Food Hydrocolloids, 2010. **24**(8): p. 744-754.
111. Danalache, F., et al., *Texture, microstructure and consumer preference of mango bars jellified with gellan gum.* LWT - Food Science and Technology, 2015. **62**(1, Part 2): p. 584-591.
112. Zhang, N., et al., *Factors affecting water resistance of alginate/gellan blend films on paper cups for hot drinks.* Carbohydrate Polymers, 2017. **156**: p. 435-442.
113. Chang, S.J., et al., *In vitro properties of gellan gum sponge as the dental filling to maintain alveolar space.* Carbohydrate Polymers, 2012. **88**(2): p. 684-689.
114. Mazzuca, C., et al., *How to tune a paper cleaning process by means of modified gellan hydrogels.* Microchemical Journal, 2016. **126**: p. 359-367.
115. Sajna, K.V., et al., *Chapter 18 - White Biotechnology in Cosmetics*, in *Industrial Biorefineries & White Biotechnology*, A. Pandey, et al., Editors. 2015, Elsevier: Amsterdam. p. 607-652.
116. Jindal, N. and J. Singh Khattar, *Chapter 4 - Microbial Polysaccharides in Food Industry*, in *Biopolymers for Food Design*, A.M. Grumezescu and A.M. Holban, Editors. 2018, Academic Press. p. 95-123.
117. M., S.S., S. Priya, and A. Maxwell, *FORMULATION AND EVALUATION OF NOVEL IN SITU GEL OF LAFUTIDINE FOR GASTRO RETENTIVE DRUG DELIVERY.* Asian Journal of Pharmaceutical and Clinical Research, 2018. **11**(8): p. 88-94.

118. Tripathi, G. and S. Singh, *Formulation and In Vitro evaluation of pH sensitive oil entrapped polymeric blended gellan gum buoyant beads of clarithromycin.* Daru : journal of Faculty of Pharmacy, Tehran University of Medical Sciences, 2010. **18**(4): p. 247-253.
119. Rajinikanth, P.S., J. Balasubramaniam, and B. Mishra, *Development and evaluation of a novel floating in situ gelling system of amoxicillin for eradication of Helicobacter pylori.* International Journal of Pharmaceutics, 2007. **335**(1): p. 114-122.
120. Rajinikanth, P.S. and B. Mishra, *Floating in situ gelling system of acetohydroxamic acid for clearance of H. pylori.* Drug Dev Ind Pharm, 2008. **34**(6): p. 577-87.
121. Meneguin, A.B., et al., *Retrograded starch/pectin coated gellan gum-microparticles for oral administration of insulin: A technological platform for protection against enzymatic degradation and improvement of intestinal permeability.* European Journal of Pharmaceutics and Biopharmaceutics, 2018. **123**: p. 84-94.
122. Vashisth, P., et al., *Ofloxacin loaded gellan/PVA nanofibers - Synthesis, characterization and evaluation of their gastroretentive/mucoadhesive drug delivery potential.* Materials Science and Engineering: C, 2017. **71**: p. 611-619.
123. Nayak, A.K., D. Pal, and K. Santra, *Tamarind seed polysaccharide-gellan mucoadhesive beads for controlled release of metformin HCl.* Carbohydrate Polymers, 2014. **103**: p. 154-163.
124. Ranch, K.M., et al., *Optimization of a novel in situ gel for sustained ocular drug delivery using Box-Behnken design: In vitro, ex vivo, in vivo and human studies.* Int J Pharm, 2019. **554**: p. 264-275.
125. Sayed, E.G., et al. *Improved corneal bioavailability of ofloxacin: biodegradable microsphere-loaded ion-activated in situ gel delivery system*. Drug design, development and therapy, 2015. **9**, 1427-1435 DOI: 10.2147/dddt.s80697.
126. Salunke, S.R. and S.B. Patil, *Ion activated in situ gel of gellan gum containing salbutamol sulphate for nasal administration.* International Journal of Biological Macromolecules, 2016. **87**: p. 41-47.
127. Patel, P. and P. Patel, *Formulation and evaluation of clindamycin HCL in situ gel for vaginal application.* International journal of pharmaceutical investigation, 2015. **5**(1): p. 50-56.
128. Carmona-Moran, C.A., et al., *Development of gellan gum containing formulations for transdermal drug delivery: Component evaluation and controlled drug release using temperature responsive nanogels.* International Journal of Pharmaceutics, 2016. **509**(1): p. 465-476.
129. Silva-Correia, J., et al., *Gellan gum-based hydrogels for intervertebral disc tissue-engineering applications.* J Tissue Eng Regen Med, 2011. **5**(6): p. e97-107.
130. Sarna, S.K., *Integrated Systems Physiology: From Molecule to Function to Disease*, in *Colonic Motility: From Bench Side to Bedside*. 2010, Morgan & Claypool Life Sciences: San Rafael (CA).
131. Bergström, J., *Experimental Characterization Techniques*. 2015. p. 19-114.
132. Polymer Properties Database. *DYNAMICAL MECHANICAL ANALYSIS*. 2021 [cited 2021 August 14th]; Available from: https://polymerdatabase.com/polymer%20physics/DMA.html.
133. Chitas R., S.C.L., Nunes C., Parreira P., Martins M.C.L., *Drug-free nanostructured lipid carriers (NLC) against Helicobacter pylori*, in *11th World Biomaterials Congress (WBC 2020)*. 2020.
134. Mudalige, T., et al., *Chapter 11 - Characterization of Nanomaterials: Tools and Challenges*, in *Nanomaterials for Food Applications*, A. López Rubio, et al., Editors. 2019, Elsevier. p. 313-353.
135. Li, Q., et al., *Dasatinib loaded nanostructured lipid carriers for effective treatment of corneal neovascularization.* Biomaterials Science, 2021. **9**.
136. Mahajan, K., et al., *Efavirenz Loaded Nanostructured Lipid Carriers for Efficient and Prolonged Viral Inhibition in HIV-Infected Macrophages.* Pharm Sci, 2021. **27**(3): p. 418-432.
137. Emami, J., H. Yousefian, and H. Sadeghi, *Targeted Nanostructured Lipid Carrier for Brain Delivery of Artemisinin: Design, Preparation, Characterization, Optimization and Cell Toxicity.* J Pharm Pharm Sci, 2018. **21**(1s): p. 225s-241s.
138. Uprit, S., et al., *Preparation and characterization of minoxidil loaded nanostructured lipid carrier gel for effective treatment of alopecia.* Saudi pharmaceutical journal : SPJ : the official publication of the Saudi Pharmaceutical Society, 2013. **21**(4): p. 379-385.
139. Guilherme, V.A., et al., *Improved efficacy of naproxen-loaded NLC for temporomandibular joint administration.* Scientific Reports, 2019. **9**(1): p. 11160.

140. Makoni, P.A., K. Wa Kasongo, and R.B. Walker, *Short Term Stability Testing of Efavirenz-Loaded Solid Lipid Nanoparticle (SLN) and Nanostructured Lipid Carrier (NLC) Dispersions*. Pharmaceutics, 2019. **11**(8): p. 397.
141. Polymer Properties Database. *MECHANICAL MODULI OF VISCOELASTIC MATERIALS*. 2021 [cited 2021 August 14th]; Available from: http://polymerdatabase.com/polymer%20physics/Modulus.html.
142. Pereira, D.R., et al., *Development of gellan gum-based microparticles/hydrogel matrices for application in the intervertebral disc regeneration.* Tissue Eng Part C Methods, 2011. **17**(10): p. 961-72.
143. Khang, G., et al., *Biological evaluation of intervertebral disc cells in different formulations of gellan gum-based hydrogels*. J Tissue Eng Regen Med, 2015. **9**(3): p. 265-75.
144. Dunson, D. *Characterization of Polymers using Dynamic Mechanical Analysis (DMA)*. 2017; Available from: https://www.eag.com/wp-content/uploads/2017/09/M-022717-Characterization-of-Polymers-using-Dynamic-Mechanical-Analysis.pdf.
145. Moorcroft, S.C.T., et al., *Nanoparticle-Loaded Hydrogel for the Light-Activated Release and Photothermal Enhancement of Antimicrobial Peptides*. ACS Applied Materials & Interfaces, 2020. **12**(22): p. 24544-24554.
146. Cleetus, C.M., et al., *Alginate Hydrogels with Embedded ZnO Nanoparticles for Wound Healing Therapy*. International journal of nanomedicine, 2020. **15**: p. 5097-5111.
147. Karoui, R., *Chapter 7 - Spectroscopic Technique: Fluorescence and Ultraviolet-Visible (UV-Vis) Spectroscopies*, in *Modern Techniques for Food Authentication (Second Edition)*, D.-W. Sun, Editor. 2018, Academic Press. p. 219-252.
148. Vigata, M., et al., *Hydrogels as Drug Delivery Systems: A Review of Current Characterization and Evaluation Techniques*. Pharmaceutics, 2020. **12**(12): p. 1188.
149. Wright, M., *Nanoparticle tracking analysis for the multiparameter characterization and counting of nanoparticle suspensions*. Methods Mol Biol, 2012. **906**: p. 511-24.
150. Gross, J., et al., *Nanoparticle tracking analysis of particle size and concentration detection in suspensions of polymer and protein samples: Influence of experimental and data evaluation parameters*. European Journal of Pharmaceutics and Biopharmaceutics, 2016. **104**: p. 30-41.
151. Fasolin, L.H., et al., *Production of hybrid gels from polysorbate and gellan gum*. Food Research International, 2013. **54**(1): p. 501-507.
152. Dave, P.N. and A. Gor, *Natural Polysaccharide-Based Hydrogels and Nanomaterials: Recent Trends and Their Applications*, in *Handbook of Nanomaterials for Industrial Applications*, C. Mustansar Hussain, Editor. 2018, Elsevier. p. 36-66.
153. Bhattarai, N., J. Gunn, and M. Zhang, *Chitosan-based hydrogels for controlled, localized drug delivery*. Advanced Drug Delivery Reviews, 2010. **62**(1): p. 83-99.
154. Narayanaswamy, R. and V.P. Torchilin, *Hydrogels and Their Applications in Targeted Drug Delivery*. Molecules, 2019. **24**(3): p. 603.
155. Rajinikanth, P.S. and B. Mishra, *Stomach-Site Specific Drug Delivery System of Clarithromycin for Eradication of Helicobacter pylori*. Chemical and Pharmaceutical Bulletin, 2009. **57**(10): p. 1068-1075.
156. Franklin-Ude, P., M. Emeje, and S. Ofoefule, *Evaluation of Gellan Gum as a Mini-Matrix for Sustained Release of Ephedrine Hydrochloride Granules*. Journal of Pharmacology and Toxicology, 2007. **2**: p. 646-652.
157. Rao, M. and S. Shelar, *Controlled Release Ion Sensitive Floating Oral in situ Gel of a Prokinetic Drug using Gellan Gum*. Indian Journal of Pharmaceutical Education and Research, 2015. **49**: p. 158-167.
158. Osmałek, T., A. Froelich, and S. Tasarek, *Application of gellan gum in pharmacy and medicine*. International Journal of Pharmaceutics, 2014. **466**(1): p. 328-340.
159. Ismail, N.A., K.A.M. Amin, and M.H. Razali, *Mechanical and Antibacterial Activities Study of Gellan Gum/Virgin Coconut Oil Film Embedded Norfloxacin*. IOP Conference Series: Materials Science and Engineering, 2018. **440**: p. 012001.
160. Lu, Y., X. Zhao, and S. Fang, *Characterization, Antimicrobial Properties and Coatings Application of Gellan Gum Oxidized with Hydrogen Peroxide*. Foods (Basel, Switzerland), 2019. **8**(1): p. 31.

161. Agnihotri, S.A., S.S. Jawalkar, and T.M. Aminabhavi, *Controlled release of cephalexin through gellan gum beads: effect of formulation parameters on entrapment efficiency, size, and drug release*. Eur J Pharm Biopharm, 2006. **63**(3): p. 249-61.